Title	Cocrystallization of nutraceuticals
Authors	Sinha, Abhijeet S.;Maguire, Anita R.;Lawrence, Simon E.
Publication date	2014-12-19
Original Citation	Sinha, A. S., Maguire, A. R. and Lawrence, S. E. (2015) 'Cocrystallization of Nutraceuticals', Crystal Growth & Design, 15(2), pp. 984-1009. doi: 10.1021/cg501009c
Type of publication	Article (peer-reviewed)
Link to publisher's version	10.1021/cg501009c
Rights	© 2014 American Chemical Society. This document is the Accepted Manuscript version of a Published Work that appeared in final form in Crystal Growth & Design, copyright © American Chemical Society after peer review and technical editing by the publisher. To access the final edited and published work see https://pubs.acs.org/doi/10.1021/cg501009c
Download date	2024-08-05 00:28:04
Item downloaded from	https://hdl.handle.net/10468/6252

Cocrystallization of nutraceuticals

Abhijeet S. Sinha,[†] Anita R. Maguire,[§] and Simon E. Lawrence[†]*

[†] Department of Chemistry, Analytical and Biological Chemistry Research Facility, Synthesis and Solid State Pharmaceutical Centre, University College Cork, Cork, Ireland

[§] Department of Chemistry and School of Pharmacy, Analytical and Biological Chemistry Research Facility, Synthesis and Solid State Pharmaceutical Centre, University College Cork, Cork, Ireland

Abstract

Cocrystallization has emerged over the past decade as an attractive technique for modification of the physicochemical properties of compounds used as active pharmaceutical ingredients (APIs), complementing more traditional methods such as salt formation. Nutraceuticals, with associated health benefits and / or medicinal properties, are attractive as coformers due to their ready availability, known pharmacological profile and natural origin, in addition to offering a dual therapy approach. Successful studies of favorably altering the physicochemical properties of APIs through cocrystallization with nutraceuticals are highlighted in this review. Many of the key functional groups commonly seen in nutraceuticals (*e.g.* acids, phenols), underpin robust supramolecular synthons in crystal engineering. This review assesses the structural data available to date across a diverse range of nutraceuticals, both in pure form and in multicomponent materials, identifies the persistent supramolecular features present. This insight will ultimately

enable predictive and controlled assembly of functional materials incorporating nutraceuticals together with APIs.

1. Introduction

Cocrystallization can be defined as bringing together two or more discrete neutral molecular species in stoichiometric amounts in a crystalline lattice, without the breaking or making of covalent bonds, utilizing non-covalent forces of interaction such as hydrogen bonds, π-π interactions, and halogen bonds.[1] These multi-component assemblies find immense use in various fields of research. Particularly within the pharmaceutical industry, they have been used for modifying the physicochemical properties of active pharmaceutical ingredients (APIs),[2-9] such as altering the aqueous solubility and/or dissolution rates,[10-13] increasing the stability,[14-16] and improving the bioavailability.[17-19] Cocrystallization is also being explored as an avenue for favorably altering the properties of agrochemicals.[20]

The choice of an appropriate coformer (cocrystal former) for APIs, which has an acceptable toxicity profile is an important aspect of co-crystallization in the pharmaceutical industry.[21] In general, the coformers are selected from the lists of generally regarded as safe (GRAS)[22] and pharmaceutically accepted salt formers.[23] Since these compounds have been previously approved by FDA,[21] utilizing them for cocrystallization reduces preclinical burden, toxicity risk and speed to clinical trials. Another class of compounds with an established safety record which can be used as viable candidates for cocrystallization in the pharmaceutical industry are the naturally occurring nutraceuticals.

Nutraceuticals, a term coined by DeFelice in 1989,[24] can be defined as, "a food (or part of a food) that provides medical or health benefits, including the prevention and/or treatment of a

disease."[24] Zeisel proposed that this was too broad and there was a need to differentiate between functional foods, nutraceuticals, and dietary supplements.[25] Accordingly, Kalra proposed the following: "a functional food which aids in the prevention and/or treatment of disease(s) and/or disorder(s) (except anemia)."[26] Common classes of nutraceuticals include polyphenols (such as phenolic acids, coumarins, stilbenes, and flavonoids),[27] and vitamins[28] (Figure 1), which form the basis used for inclusion in this review.

Gallic acid (phenolic acid)　　Quercetin (flavonoid)　　Nicotinic acid (vitamin B3)
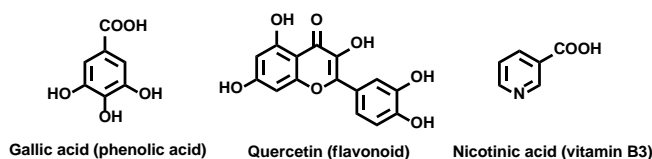
Figure 1. Common classes of nutraceuticals.

The area of research on nutraceuticals is an evergrowing field, not only due to the potential health benefits associated with this class of compounds, but also because of their perceived therapeutic effect in multiple areas of medicine such as pain killers, cold and cough, sleeping disorders, digestion, and prevention of certain cancers.[29,30] Also, the fact that they are patentable (meet the criteria required for patents), coupled with them being readily available over the counter, has led to an increased use of nutraceuticals as coformers in the pharmaceutical industry.[31] The synergistic effect of nutraceuticals and APIs can be utilized to improve the poor physicochemical properties, such as stability,[32] solubility[33-35] and bioavailability,[36] in a bid to assemble safe materials with improved properties. Also, the anti-oxidant properties of nutraceuticals can be used to impart stability to APIs that are prone to oxidation. Additionally, nutraceuticals with known health benefits but poor physicochemical properties can be co-crystallized with GRAS acceptable coformers.[37,38]

Cocrystallization of nutraceuticals is an important area of current research and holds tremendous potential for the future, as indicated by the rise in the number of cocrystals of nutraceuticals over the past few years based on the data obtained from the Cambridge Structural Database (CSD).[39,40] Pharmaceutical cocrystals have been extensively reviewed.[2,32,33,37] Despite the rapidly increasing number of crystallographic studies of nutraceuticals, and a review of their structural chemistry and behavioral patterns in the solid-state has not yet been clearly detailed. The one review to date on nutraceutical cococrytals exclusively focused on their physicochemical properties.[31] In this review, we detail the different known forms of two different classes of nutraceuticals, namely polyphenols and vitamins. We examine the specific intra- and intermolecular interactions present in their crystal structures. We also analyze the findings in conjunction with the general solid-state behavior of the specific functional groups present within each class of nutraceuticals. Finally, we highlight some of the pharmaceutically relevant studies conducted over the past decade on improving the physicochemical properties of APIs via cocrystallization with nutraceuticals.

The Cambridge Structural Database (CSD) (ConQuest v. 1.16, May 2014 update) was used to obtain information about the crystal structures of the various nutraceuticals and the following filters were applied to the searches to limit the results: 3D coordinates determined, R factor < 7.5 %, no ions and only organics. The review has been organized around three categories: (i) phenolic acids (Figure 2); (ii) polyphenols including coumarin, stilbenes, flavonoids and lignans (Figure 3); and (iii) vitamins (Figure 4). The first two categories are members of the polyphenol family, differing only in the functional groups present in the molecules. Within each category, the data mined from the CSD was split up into six different groupings to facilitate the understanding of the nature of the intra- and intermolecular

interactions that are present in these molecules: (a) pure compounds; (b) hydrates; (c) cocrystals; (d) hydrated cocrystals; (e) salts; and (f) solvates (Table 1).
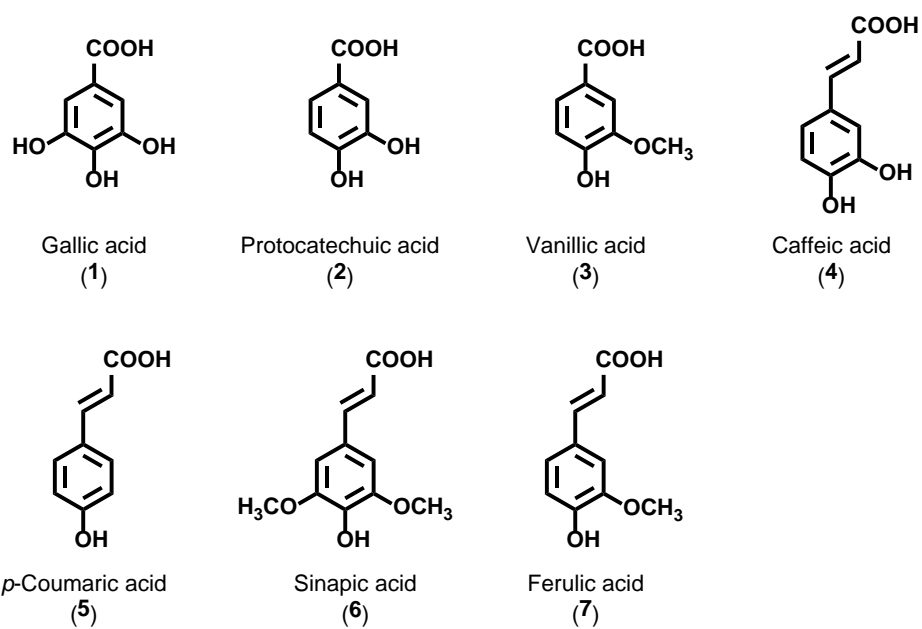

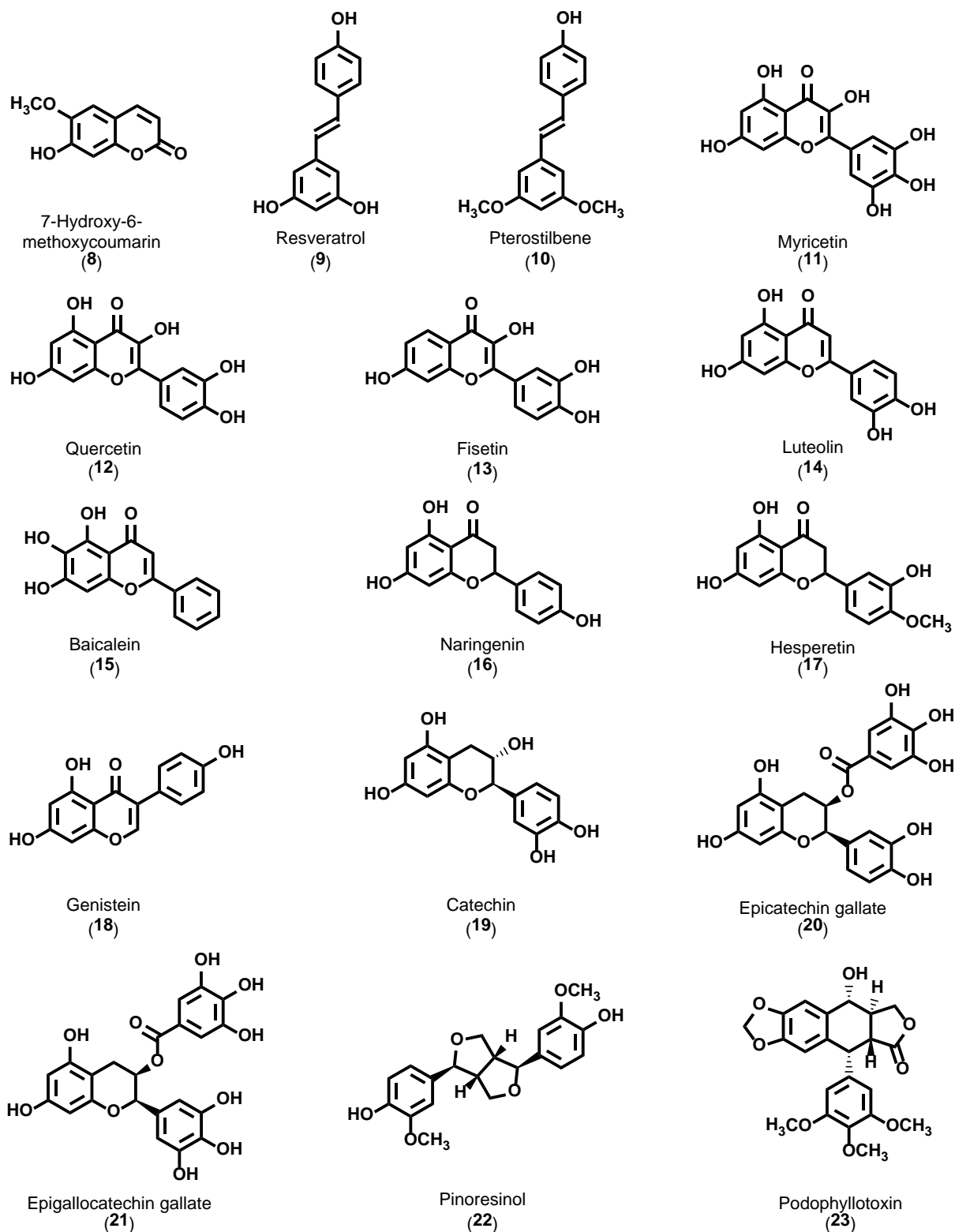**Figure 2.** Structures of the phenolic acids examined.

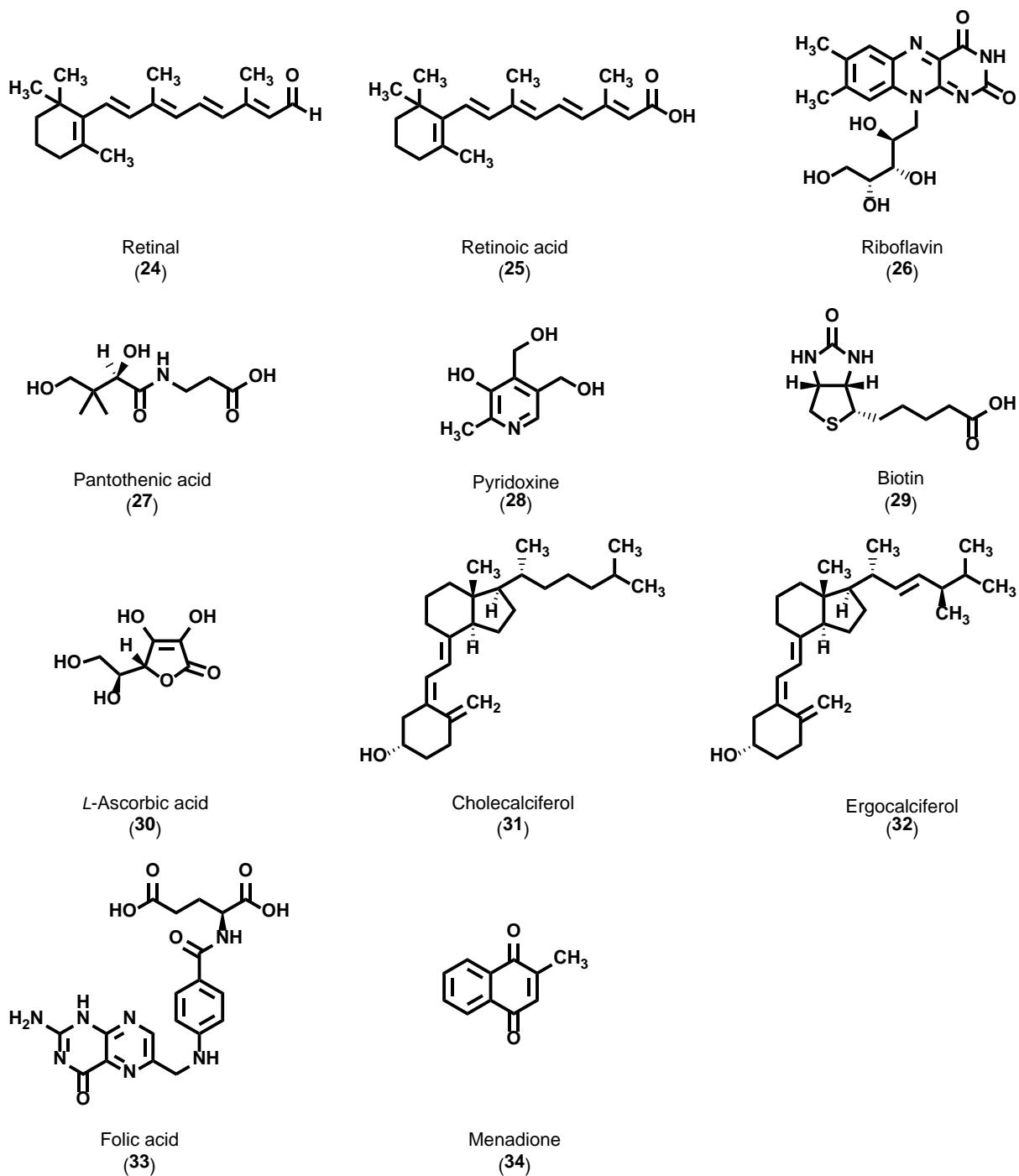**Figure 3.** Structures of the polyphenols examined, consisting of coumarin (**8**), stilbenes (**9**-**10**), flavonoids (**11**-**21**) and lignans (**22**-**23**).

Retinal
(**24**)

Retinoic acid
(**25**)

Riboflavin
(**26**)

Pantothenic acid
(**27**)

Pyridoxine
(**28**)

Biotin
(**29**)

L-Ascorbic acid
(**30**)

Cholecalciferol
(**31**)

Ergocalciferol
(**32**)

Folic acid
(**33**)

Menadione
(**34**)

Figure 4. Structures of the vitamins examined.

Table 1. Solid-state forms observed for the nutraceuticals.

Molecule	Structure	Hydrated structures	Cocrystals	Hydrated cocrystals	Salts	Solvates[i]
Gallic acid, **1**	3	5	9	5	4	2
Protocatechuic acid, **2**	1	3	3	0	1	2
Vanillic acid, **3**	1	0	4	0	0	0
Caffeic acid, **4**	1	0	0	1	0	0
p-Coumaric acid, **5**	1	0	6	1	1	1
Sinapic acid, **6**	0	0	0	0	0	1
Ferulic acid, **7**	1	0	2	2	1	0
7-Hydroxy-6-methoxycoumarin, **8**	2	0	0	0	0	0
Resveratrol, **9**	1	0	0	0	1	0
Pterostilbene, **10**	0	0	5	0	0	0
Myricetin, **11**	0	0	2	0	0	0
Quercetin, **12**	0	2	2	1	1	2
Fisetin, **13**	0	0	1	0	0	1
Luteolin, **14**	0	1	2	0	0	0
Baicalein, **15**	1	0	1	0	0	0
Naringenin, **16**	1	0	0	0	0	0
Hesperetin, **17**	1	1	0	0	2	0
Genistein, **18**	1	0	1	1	0	0
Catechin, **19**	1	1	0	2	0	2
Epicatechin gallate, **20**	0	0	0	2	0	0
Epigallocatechin gallate, **21**	1	1	0	7	1	2
Pinoresinol, **22**	2	0	0	0	0	2
Podophyllotoxin, **23**	2	0	0	0	0	3
Retinal, **24**	5	0	0	0	0	0
Retinoic acid, **25**	3	0	1	0	0	0
Riboflavin, **26**	0	0	0	2	2	0
Pantothenic acid, **27**	0	0	0	0	1	0
Pyridoxine, **28**	1	0	0	0	5	0
Biotin, **29**	1	0	0	0	0	0
Ascorbic acid, **30**	2	0	0	0	5	0
Cholecalciferol, **31**	1	0	2	0	0	0
Ergocalciferol, **32**	1	0	1	0	0	0

| Folic acid, **33** | 0 | 1 | 0 | 0 | 0 | 0 |
| Menadione, **33** | 2 | 0 | 0 | 0 | 0 | 0 |

[i] Solvates of the nutraceuticals and their cocrystals are included in this category.

2. Polyphenols

Natural polyphenols are arguably the largest class of nutraceuticals which are commonly found in fruits, vegetables, tea, and barks of medicinal plants.[27] Not only do they possess scavenging properties towards radical oxygen species, but are also capable of complexing with proteins.[41] As a result, they are interesting candidates for the treatment of various symptoms and diseases such as inflammation or cancer, and for anti-ageing purposes in cosmetic formulations.[42,43] However, their use in any pharmaceutical applications is limited by their low aqueous solubility and poor stability, generally being sensitivity to light and heat.[27] Different techniques such as encapsulation and cocrystallization have been employed to improve the physicochemical properties of polyphenols, to aid in increasing their use in the pharmaceutical industry. [27]

2.1. Phenolic acids

The crystal structures for all the phenolic acids except sinapic acid are known. In two cases (**1**-**2**), hydrated structures of the molecules by themselves are observed. A total of 24 cocrystals were observed for these molecules, with a maximum of nine cocrystals observed for gallic acid (**1**). There were nine structures where the nutraceuticals formed hydrated cocrystals in the presence of other hydrogen-bond donor or acceptor molecules, whereas in four cases, the formation of salts was observed (**1**-**2**, **5**, **7**). The crystal structures were examined in detail and are described below.

Focusing initially on gallic acid, the simple planar compound combining carboxylic acid and phenolic moieties displays remarkable versatility in terms of its co-crystallization behavior

with co-formers or indeed solvates. The solid state structure of gallic acid on its own displays characteristic chains of $R_2^2(8)$ dimers (using graph set notation)[44,45] linked through the *p*-hydroxy groups with interlinking orthogonal chains in 3-D through the remaining phenolic units (IJUMEG04) (Figure 5).[46]
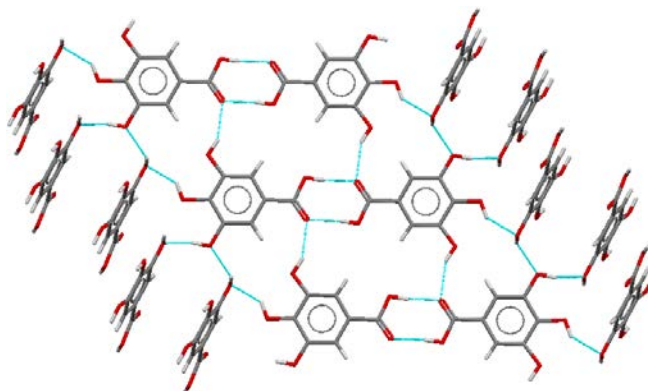

Figure 5. The structure of gallic acid (IJUMEG04). [46]

Interestingly, in the many hydrate forms while the $R_2^2(8)$ dimer is retained in some of the structures, it is absent in others, and versatile hydrogen bonds to water through the phenolic groups are clearly feasible in the solid state.[46-49] Thus, the multiple hydrogen bonds between the phenols and the water molecules can compensate for the carboxylic acid dimer. The existence of 5 hydrates of gallic acid (KONTIQ, KONTIQ01, KONTIQ04, KONTIQ05, and KONTIQ06)[46-49] and 5 polymorphs of the acetamide-gallic acid cocrystal (1:1 in PEFGEO, PEFGEO01, PEFGEO02 and PEFGEO03; 1:3 in PEFGIS)[50] in which a blend of acid-acid and acid-amide dimer is seen highlights the flexibility of gallic acid as a co-former for APIs, and this is further evidenced by co-crystals of gallic acid with oxiracetam (1:1 in ZEBXEL and ZEBXIP)[51] (Figure 6) and isoniazid (1:1 in LODHOD)[52] (Figure 7). Of the co-crystals observed, the intermolecular interactions such as acid-amide, acid-pyridyl, acid-heterocyclic amine, acid-*N*-oxide, clearly compete for the acid-acid homodimer, as would be expected based on Etter's rules.[44,53-55] In

other cases, the acid-acid dimer persists with the co-former forming hydrogen bonds to the phenol moieties essentially capping the dimer motifs.
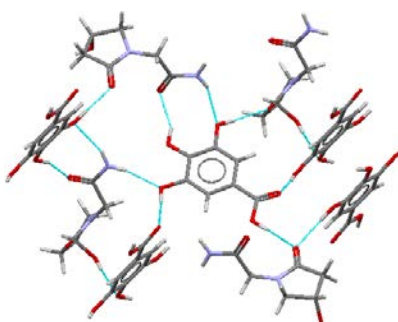
Figure 6. The structure of 1:1 gallic acid-oxiracetam cocrystal (ZEBXEL).[51]
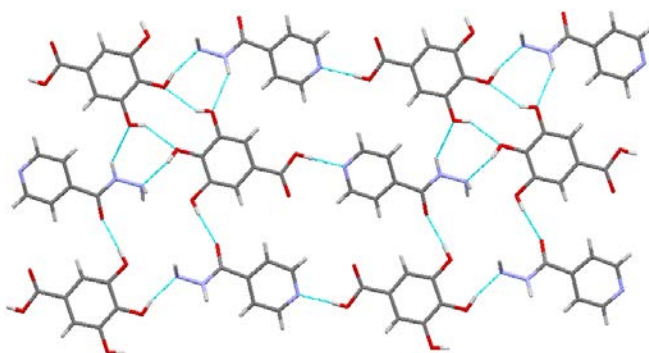
Figure 7. The structure of 1:1 gallic acid-isoniazid cocrystal (LODHOD).[52]

There are ten known crystal structures containing protocatechuic acid (see Table 1). An examination of the structure of protocatechuic acid by itself reveals that the acid moiety is forming the well-known $R_2^2(8)$ acid-acid dimer which is capped on both ends by a phenolic substituent of protocatechuic acid *via* O-H$^{...}$O hydrogen bonds (WUYNUA) (Figure 8).[56] At the other end six phenolic substituents from four adjacent protocatechuic acid molecules are forming an extended $R_4^2(14)$ supramolecular synthon,[57] thus giving rise to an extended architecture.
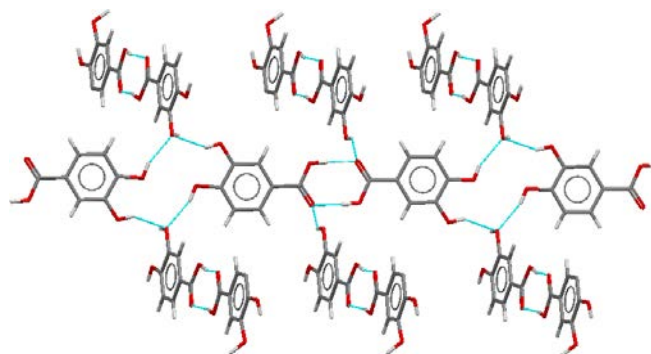
Figure 8. The structure of protocatechuic acid (WUYNUA).[56]

There are three polymorphs of protocatechuic acid monohydrate (BIJDON03, BIJDON04 and BIJDON05), and they all retain identical supramolecular motifs to the structure of protocatechuic acid by itself. The expected $R_2^2(8)$ acid-acid dimer is retained, whereas the phenol groups capping the acid dimer has been replaced by water molecules capping the acid-acid dimer (Figure 9).[56,58,59] In one of the polymorphs two water molecules and four phenolic substituents from two adjacent protocatechuic acid molecules are forming a similar $R_4^2(14)$ supramolecular synthon to the one observed in protocatechuic acid (BIJDON03).[58]
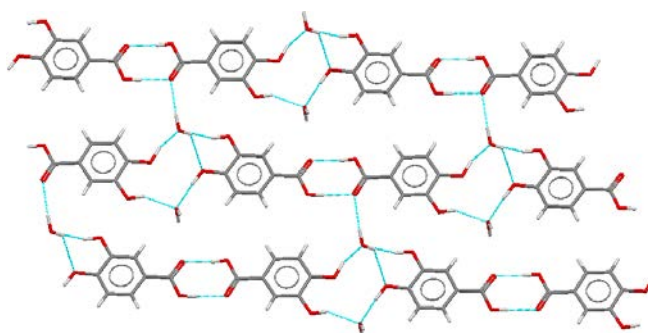
Figure 9. The structure of protocatechuic acid monohydrate (BIJDON03).[58]

An examination of the structure of protocatechuic acid-oxiracetam (1:1) cocrystals reveals that the acid-acid homodimer has been replaced by the acid-amide heterodimer (ZEBXOV and ZEBXUB) (Figure 10).[51] Also, one of the phenolic substituents is extending the

12

motif into 1-D ribbons *via* O-H⋯O hydrogen bonds between the phenol group of the protocatechuic acid and the alcohol group of the oxiracetam. Furthermore, the other phenolic substituent caps the acid-amide dimer *via* phenol O-H⋯O=C carbonyl hydrogen bonds, where the supramolecular architecture is further extended *via anti*-amide N-H⋯O alcohol intermolecular interactions between two oxiracetam molecules.
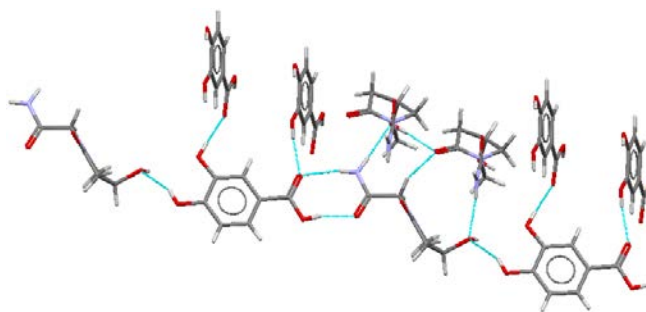
Figure 10. The structure of 1:1 protocatechuic acid-oxiracetam cocrystal (ZEBXOV).[51]

The structure of vanillic acid displays the familiar acid-acid homodimer and the only phenolic substituent caps the hydroxyl moiety of the acid-acid dimer on both ends, thus giving rise to 2-D sheets (CEHGUS) (Figure 11).[60]
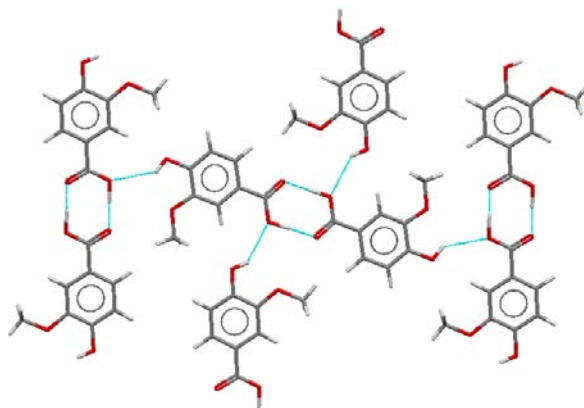
Figure 11. The structure of vanillic acid (CEHGUS).[60]

The vanillic acid-pyrazine-2-carboxamide (1:1) cocrystal surprisingly displays separate acid-acid and amide-amide homodimers for vanillic acid and pyrazine-2-carboxamide

13

respectively (REBXED), Figure 12, in contrast to the more usual acid-amide heterodimer. [61] The two discrete dimers are interlinked *via* phenol O-H$\cdots$N$_{arom}$ hydrogen bonds and a R$_2^2$(10) ring formed *via* *anti*-amide N-H$\cdots$N$_{arom}$ hydrogen bonds between two adjacent pyrazine-2-carboxamide molecules, thus giving rise to a supramolecular architecture resembling 2-D sheets.
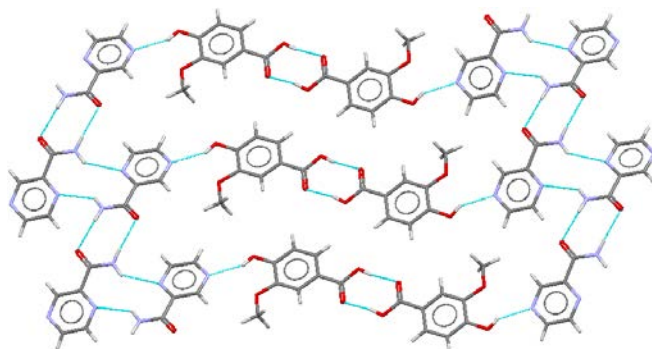
Figure 12. The structure of 1:1 vanillic acid-pyrazine-2-carboxamide cocrystal (REBXED). [61]

The 1:1 cocrystal of vanillic acid with the API ethenzamide shows the formation of the favored acid-amide heterodimer with the only phenolic substituent on vanillic acid capping the carbonyl of the acid moiety in the acid-amide dimer (REHSII) (Figure 13).[62] A similar heterodimer supramolecular motif is also observed in the cocrystal between vanillic acid and 4-chloro-3,5-dimethyl-1H-pyrazole (1:1), wherein the acid moiety is hydrogen bonded to the pyrazole moiety forming an R$_2^2$(7) dimer with the phenolic substituent capping the acid carbonyl group (PEKWUZ). [63]
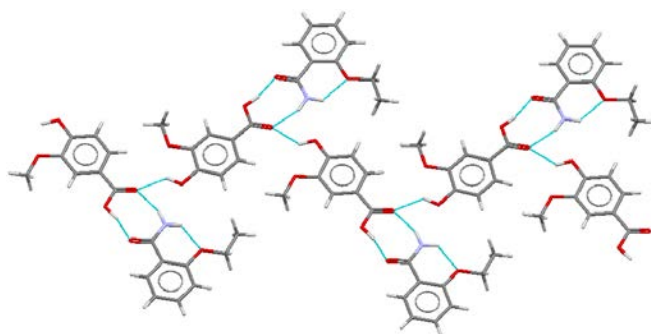
Figure 13. The structure of 1:1 vanillic acid-ethenzamide cocrystal (REHSII). [62]

Another novel 1:1 cocrystal of vanillic acid with the bioactive herbal medicine andrographolide displays the hydroxy lactone moiety of adjacent andrographolide molecules connected through strong alcohol O-H···O=C hydrogen bonds leading to the formation of 1-D tapes (GIHCIL) (Figure 14).[64] Vanillic acid molecules connect these 1-D tapes *via* phenol/acid O-H···O alcohol hydrogen bonds on both sides. Notably, the acid-acid dimer is absent in this supramolecular architecture.
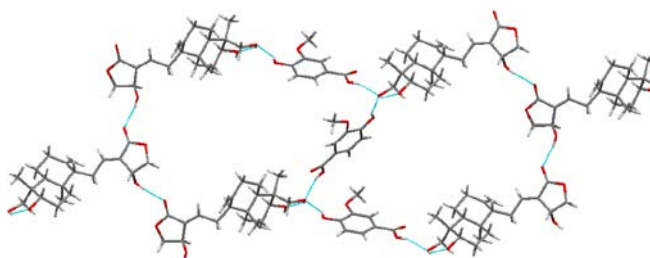
Figure 14. The structure of 1:1 vanillic acid-andrographolide cocrystal (GIHCIL). [64]

The structure of caffeic acid displays identical motifs to those observed in gallic acid and protocatechuic acid, wherein the expected acid-acid homodimer is retained with one of the phenolic substituents responsible for satisfying the carbonyl group of the acid-acid dimer on both sides (FESNOG01) (Figure 15).[65] The remaining phenolic substituent forms bifurcated hydrogen bonds with two phenolic substituents of an adjacent caffeic acid molecule.
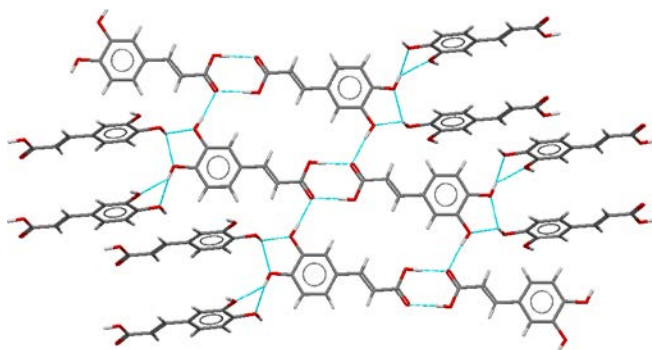
Figure 15. The structure of caffeic acid (FESNOG01).[65]

The structure of caffeic acid-nicotinamide (1:1) monohydrate also displays the preferred acid-amide heterodimer, where the two phenolic substituents of caffeic acid on adjacent molecules are involved in forming a $R_2^2(10)$ supramolecular homosynthon, thus giving rise to a 2-D sheet like architecture (MUPMOA) (Figure 16).[66] This is further extended to a 3-D supramolecular architecture due to the water molecules acting as a bridge between two adjacent layers *via* water O-H$\cdots$N$_{arom}$ and water O-H$\cdots$O phenol hydrogen bonds.
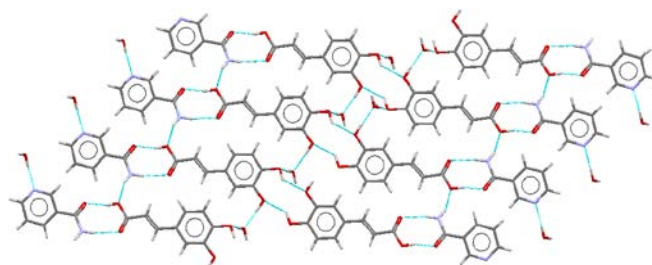
Figure 16. The structure of caffeic acid-nicotinamide (1:1) monohydrate (MUPMOA).[66]

There are ten known crystal structures containing *p*-coumaric acid (see Table 1). An examination of the structure of *p*-coumaric acid by itself reveals two interesting features: (a) presence of the $R_2^2(8)$ acid-acid homodimer; and (b) formation of the phenol C(2) catemeric chains (COUMAC01) (Figure 17).[67] A notable observation here is the absence of the discrete

16

phenol O-H⋯O=C hydrogen bonds which are prevalent in the structures of the other phenolic acids (**1**-**4**, **7**).
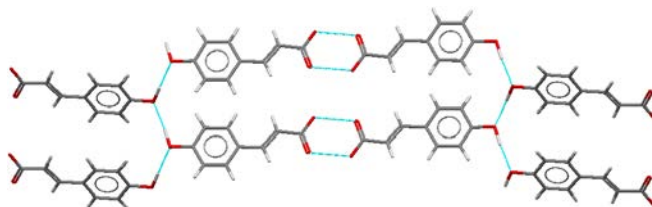
Figure 17. The structure of *p*-coumaric acid (COUMAC01).[67]

The acid-acid homodimer in *p*-coumaric acid has been replaced by acid O-H⋯N$_{arom}$ hydrogen bonds in the structure of *p*-coumaric acid-caffeine (1:1) cocrystal (IJEZUT) (Figure 18).[68] At the other end of the molecule the phenolic substituent is forming intermolecular hydrogen bonds with one of the carbonyl groups on caffeine, thus giving rise to 1-D chains. The corresponding *p*-coumaric acid-caffeine (1:2) hydrated complex retains the same supramolecular motifs in its structure, with the only difference being the absence of 1-D chain like architecture in the hydrated complex (IJIBAF).[68]

Figure 18. The structure of *p*-coumaric acid-caffeine (1:1) cocrystal (IJEZUT).[68]

The two known polymorphs of the 1:1 cocrystal of *p*-coumaric acid with the respiratory drug theophylline display synthon polymorphism, where both Form I (IJIBEJ) and II (IJIBEJ01) possess a $R_2^2(9)$ carboxylic acid-imidazole heterosynthon.[68] However, in Form I the phenolic substituent on *p*-coumaric acid is forming hydrogen bonds with the remaining carbonyl group on

theophylline (Figure 19), whereas, in Form II the phenolic substituent on *p*-coumaric acid is hydrogen bonded to the imidazole nitrogen atom of theophylline (Figure 20).
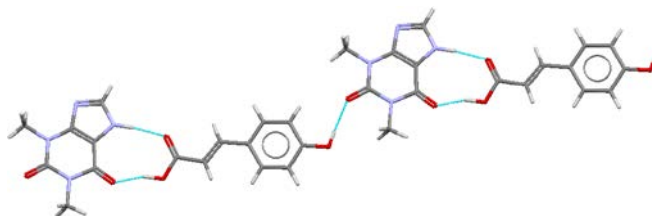

Figure 19. The structure of *p*-coumaric acid-theophylline (1:1) cocrystal, Form I (IJIBEJ).[68]
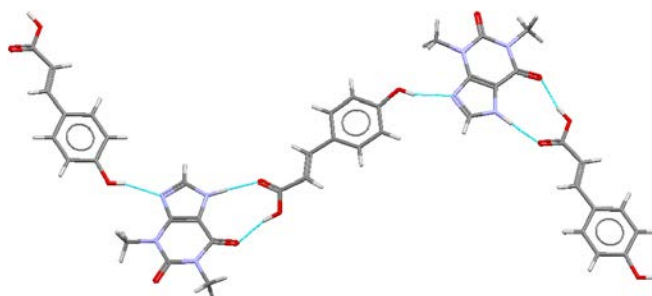

Figure 20. The structure of *p*-coumaric acid-theophylline (1:1) cocrystal, Form II (IJIBEJ01).[68]

The structure of the 1:1 cocrystal of *p*-coumaric acid with the API isonicotinohydrazide displays the expected $R_2^2(7)$ acid-hydrazide heterosynthon (PEHFUF) (Figure 21).[69] This motif is extended into 1-D ribbons by hydrogen bonds between the phenolic substituent of *p*-coumaric acid and the aromatic nitrogen atom of isonicotinohydrazide. Furthermore, adjacent ribbons are interlinked *via* hydrogen bonds between the *anti*-hydrazide hydrogen atom and the carbonyl of the acid, thus giving rise to a 2-D sheet like supramolecular architecture.
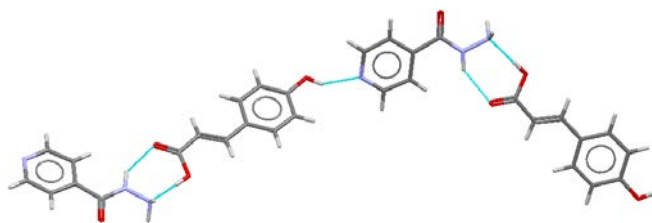
Figure 21. The structure of *p*-coumaric acid-isonicotinohydrazide (1:1) cocrystal (PEHFUF).[69]

There are three polymorphs of the 1:1 cocrystal of *p*-coumaric acid with nicotinamide, of which only Forms I (SOLBEC01) and III (SOLBEC) have been characterized by single crystal X-ray diffraction.[70] Both of these forms display identical primary intermolecular interactions, *i.e.* the preferred acid-amide heterosynthon coupled with the phenol O-H$^{...}$N$_{arom}$ hydrogen bonds are responsible for the formation of 1-D chains in both cases. The striking difference between the two structures is the crosslinking hydrogen bonds present between adjacent 1-D chains. In Form I the *anti*-amide hydrogen atom is hydrogen bonded to the hydroxyl oxygen atom of the acid moiety (Figure 22), whereas in Form III two *anti*-amide hydrogen atoms coupled with the carbonyl oxygen atoms of the acid moiety are forming a complementary $R_4^2(8)$ supramolecular synthon (Figure 23).[70]
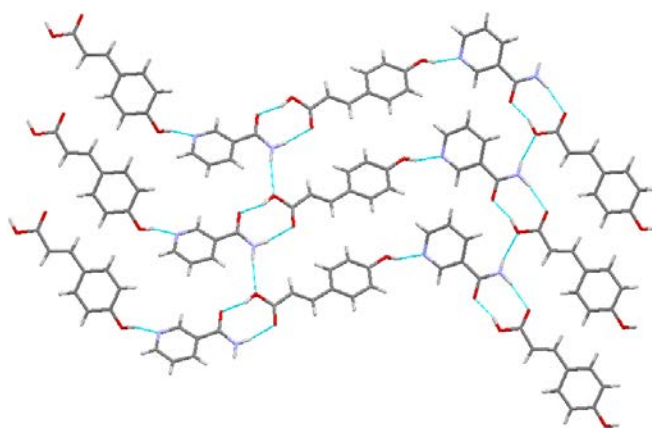
Figure 22. The structure of *p*-coumaric acid-nicotinamide cocrystal (Form I) (SOLBEC01).[70]
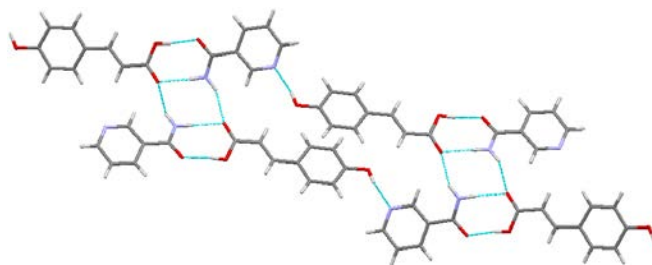
Figure 23. The structure of *p*-coumaric acid-nicotinamide cocrystal (Form III) (SOLBEC).[70]

The structure of ferulic acid displays identical supramolecular motifs to those observed in vanillic acid, *i.e.* the acid-acid homodimer is retained along with the hydrogen bond between the phenolic substituent and the hydroxy moiety of an adjacent acid-acid dimer (GASVOL01) (Figure 24).[71] The similarity between the two acids can be attributed to the presence of an identical aromatic backbone in both molecules (*meta* methoxy and *para* hydroxy substituents).
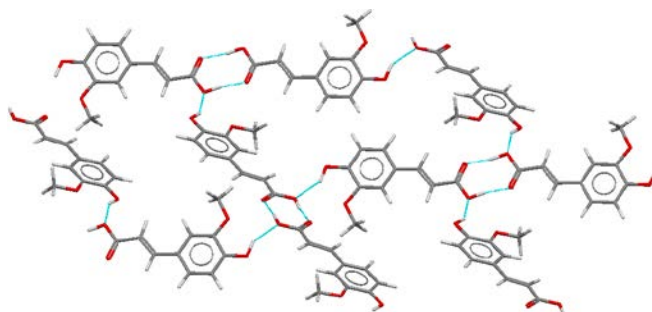
Figure 24. The structure of ferulic acid (GASVOL01).[71]

There are two cocrystals of ferulic acid (IKAFAC and BUFQAO)[72,73] of which the 1:1:1 ternary cocrystal of ferulic acid with 3,5-dinitrobenzoic acid and isonicotinamide is a classic example of Etter's rules in hydrogen bonding being used to assemble complex supramolecular architectures (BUFQAO). The primary hydrogen bond donor is the acid moiety of 3,5-dinitrobenzoic acid which is hydrogen bonding with the primary hydrogen bond acceptor *i.e.* the pyridyl nitrogen atom of isonicotinamide (O-H···N 1.366 Å, HO···N 2.559 Å, O-H···N 174.59º) (Figure 25).[72] The secondary hydrogen bond donor and acceptor are the acid moiety of ferulic

acid and the amide end of isonicotinamide which are forming an acid-amide heterodimer (O-H···O 1.658 Å, HO···O 2.636 Å, O-H···O 171.10º; N-H···O 1.827 Å, HN···O 2.819 Å, N-H···O 167.71º). The extended architecture is assembled *via* ferulic acid phenol O-H···O=C carbonyl 3,5-dinitrobenzoic acid (O-H···O 1.908 Å, HO···O 2.714 Å, O-H···O 128.58º) and *anti*-amide N-H···O nitro hydrogen bonds. The selectivity in terms of hydrogen bonds is also reflected in the observed hydrogen bonding distances.
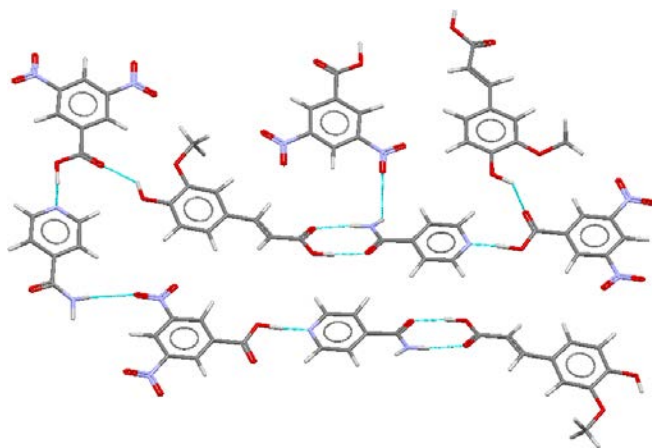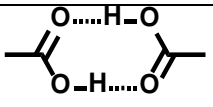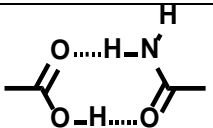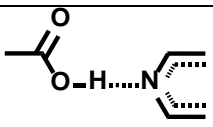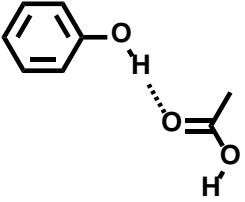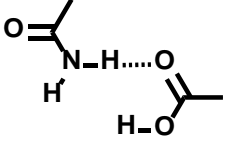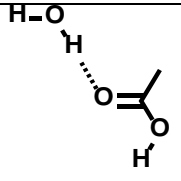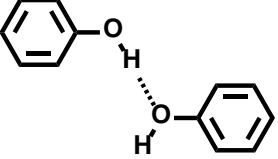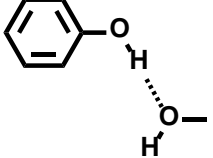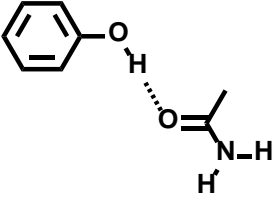

Figure 25. The structure of 1:1:1 ferulic acid-isonicotinamide-3,5-dinitrobenzoic acid ternary cocrystal (BUFQAO).[72]

2.1.1 Common features observed for phenolic acids

Some common structural features that are observed in the structures of different phenolic acids along with the robust intermolecular interactions, Table 2, which are present in these crystal structures are outlined in this section.

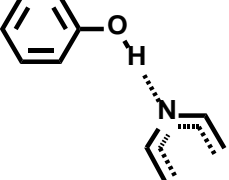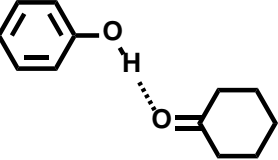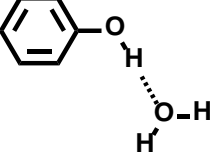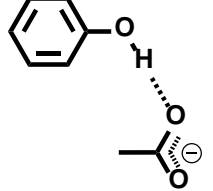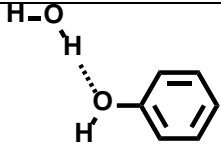**Table 2.** The most common intra- and intermolecular interactions observed in the phenolic acids have been organized in four categories: (i) acids as donors; (ii) acids as acceptors; (iii) phenols as donors; and (iv) phenols as acceptors.

Type of Interaction	Structure	Hydrated structures	Cocrystals	Hydrated cocrystals	Salts	Solvates
Acids as donors						
O·····H–O / O–H·····O (carboxylic acid dimer)	**1**(3), **2, 3, 4, 5, 7**	**1**(3), **2**(3)	**1**(2), **3, 7**	**1**	**1**(2), **2**	**2, 6**
O·····H–N / O–H·····O (amide interaction)			**1**(3), **2**(2), **3, 5**(2), **7**	**1, 4, 7**(2)		
O / O–H·····N (pyridine acceptor)			**1, 3, 5, 7**	**1**(2), **5**		**1**(2), **2, 5**
Acids as acceptors						
(phenol···O=C–O–H)	**1**(3), **2, 4**	**1**(5)	**1**(3), **2**(2), **3**(2), **7**	**1**	**1**	**1**(2), **2**
O=C–N–H·····O / H–O			**1**(4)	**1**		
H–O···O=C–O–H		**2**(3)		**1**	**1**	
Phenols as donors						

	1(3), **2**, **4**, **5**	**1**(4), **2**(2)	**1**(5), **2**	**1**, **4**		**1**, **2**(2)
			2(2), **3**			**1**, **5**, **6**
			1(7)	**1**(2)		
			1, **3**, **5**(4), **7**	**1**(2)		**1**
			1(2)	**1**(2)		
		1(5), **2**(3)		**1**(5), **4**, **7**(2)	**1**(3), **2**, **5**	**5**
					1(4), **2**, **7**	
Phenols as acceptors						

		1(5), **2**(3)		**1**(3), 4, 7	**1**(2), **2**, **7**	

Numbers in brackets indicate the number of times the particular interaction is observed in the appropriate compound (as identified in Figure 2).

It is observed that the structures of all the phenolic acids as pure compounds display three characteristic types of intermolecular interactions: (a) acid···acid dimer (**1**-**5**, **7**); (b) phenol O-H···O phenol hydrogen bonds (**1**-**2**, **4**-**5**); and (c) phenol O-H···O=C acid discrete hydrogen bonds (**1**-**2**, **4**) (Figure 26).

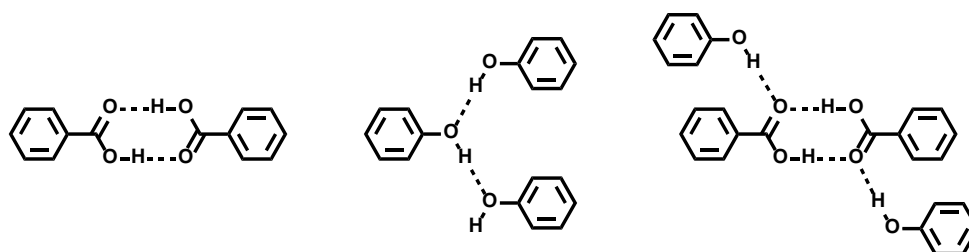**Figure 26.** The three common hydrogen bonding motifs observed in phenolic acids: (a) acid···acid dimer (left); phenol O-H···O phenol (middle) and phenol O-H···O=C acid discrete hydrogen bonds (right).

These observations are in accordance with the data from the CSD on carboxylic acids,[74] where in the absence of competing hydrogen bond donors or acceptors, the carboxylic acid moiety will preferentially form the homodimer supramolecular synthon (Table 2). Similarly, the phenolic substituents exhibit the common motifs associated with phenols such as the phenol O-H···O phenol homosynthon or the phenol O-H···O=C acid heterosynthon.[75-77] A notable observation is that as the number of phenolic substituents on the phenolic acid backbone increase, other hydrogen bonding synthons characteristic of the phenol functional group become more prevalent and all the phenolic substituents are involved in hydrogen bonding. For example,

24

a higher number of hydrates are seen for gallic acid (**1**) and protocatechuic acid (**2**) which have three and two phenolic substituents respectively. This can be a direct consequence of an increase in the number of unsatisfied hydrogen bond donors and acceptors as the number of phenolic substituents increases, and thus other intermolecular interactions such as phenol O-H···O water and water O-H···O phenol hydrogen bonds are seen.

Upon cocrystallization the acid-acid homodimer gives way to the favored heteromeric synthons such as acid-amide and acid-N_{arom} supramolecular motifs, whereas the phenolic substituents are involved in phenol O-H···O phenol, phenol O-H···O=C acid, phenol O-H···O=C amide and phenol O-H···N_{arom} hydrogen bonds.[75,78,79] The observed motifs for the acid and phenol moieties are representative of the coformer used and the functional groups present in the coformers.

Consideration of the calculated molecular electrostatic potentials (MEPs) for the phenolic acids should allow for a better understanding of the hydrogen bonding capability of acids and phenols.[80] Accordingly, charge calculations were performed, using Spartan'14 (Wavefunction, Inc. Irvine, CA). All molecules were energy optimized using DFT B3LYP/6-31+G* *ab initio* calculations, with the maxima and minima in the electrostatic potential surface (0.002 e au^{-1} iso-surface) determined using a positive point charge in vacuum as a probe. Based on the calculated MEPs, the phenols are a more effective hydrogen bond donor than the acid moiety as observed in compounds **1**-**5**, see Figure 27, and thus in a competitive molecular recognition situation should compete effectively with acids for available hydrogen bond acceptors. The two exceptions are **6**-**7**, where the presence of the electron donating methoxy groups on the aromatic ring are responsible for decreasing the calculated MEP values of the phenolic moiety. In the two examples of cocrystals of phenolic acids with either a symmetric ditopic hydrogen bond acceptor

(WAJWAH) (acid O-H⋯O 1.81 Å, HO⋯O 2.624(5) Å, O-H⋯O 175.4°; phenol O-H⋯O 1.81 Å, HO⋯O 2.629(4) Å, O-H⋯O 177.3°),[81] or an asymmetric ditopic hydrogen bond acceptor (WAJXAI) (acid O-H⋯O 1.84 Å, HO⋯O 2.655(2) Å, O-H⋯O 173.7°; phenol O-H⋯O 1.84 Å, HO⋯O 2.647(3) Å, O-H⋯O 166.0°; phenol O-H⋯N 2.00 Å, HO⋯N 2.707(3) Å, O-H⋯N 144.5°),[81] the two functional groups compete with each other for the available hydrogen bond acceptors (also reflected in the observed hydrogen bonding distances), and thus hydrogen bonding occurs with both ends of the molecule. A more detailed study with multiple monotopic / ditopic symmetric / ditopic asymmetric hydrogen bond acceptors is required to shed further light on the existing competition in hydrogen bonding between phenols and acids, and correlate the observed interactions with the predicted interactions based on the calculated MEPs.
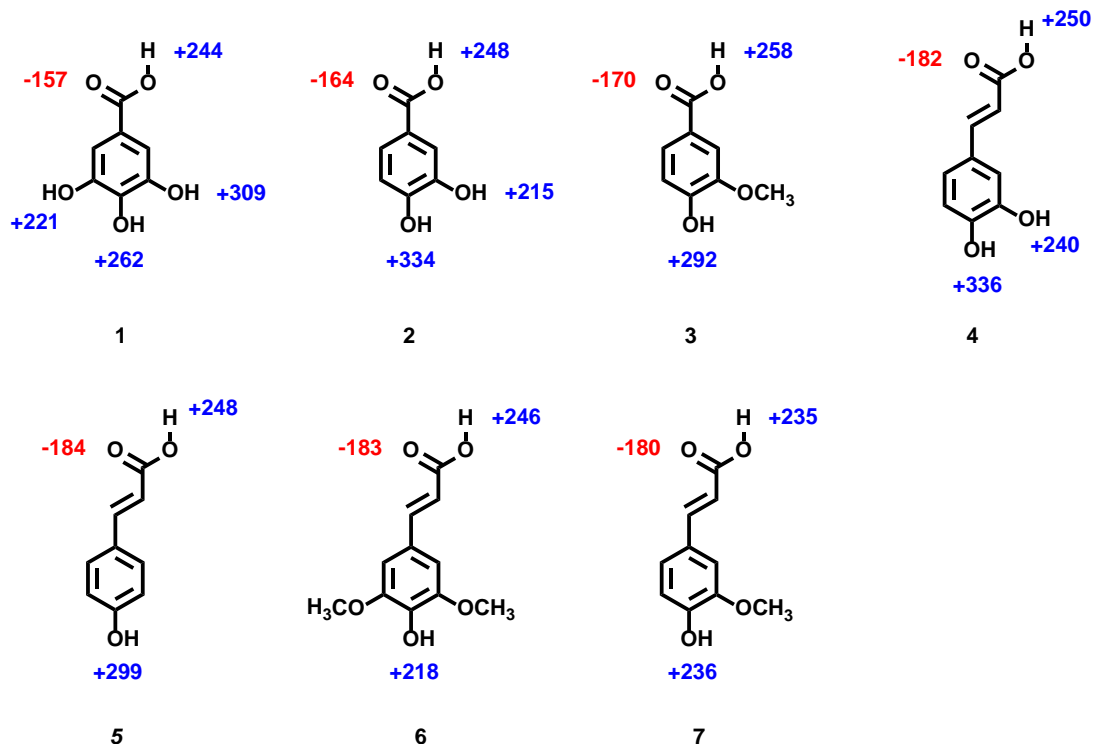

Figure 27. The calculated molecular electrostatic potentials (kJ mol^{-1}) for the phenolic acids. Blue = positive potential, red = negative potential.

2.2. Polyphenols (including coumarin, stilbenes, flavonoids and lignans)

Polyphenols such as coumarins, stilbenes, flavonoids and lignans are widely found in the plant kingdom.[82] They are very potent antioxidants *in vitro*, and as a result have been known to exhibit several biological effects such as protection against cardiovascular diseases, anti-hepatotoxic, anti-inflammatory and anti-ulcer activities.[83] This has led to an increased interest in the pharmaceutical properties and applications of polyphenols over the past decade. Sixteen different molecules have been explored in this category, of which one is a coumarin (**8**), two are stilbenes (**9-10**), eleven flavonoids [three flavonols (**11-13**), two flavones (**14-15**), two flavanones (**16-17**), one isoflavone (**18**), three flavanols/catechins (**19-21**)], and finally two lignans (**22-23**) have been included (Figure 3).

7-Hydroxy-6-methoxycoumarin is a simple planar molecule with a single hydrogen bond donor in the form of the phenolic substituent. Both polymorphs exhibit the same 1-D chains *via* phenol O-H···O=C hydrogen bonds (HXMCOU and HXMCOU01) (Figure 28).[84,85]
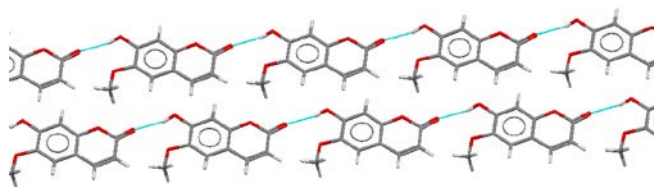

Figure 28. One polymorph of 7-hydroxy-6-methoxycoumarin (HXMCOU).[84]

There are two known crystal structures containing resveratrol (see Table 1). An examination of the structure of resveratrol by itself reveals the formation of multiple phenol O-H···O phenol C(2) catemeric chains between the three phenolic substituents in the absence of any other hydrogen bond donors or acceptors (DALGON) (Figure 29).[86]
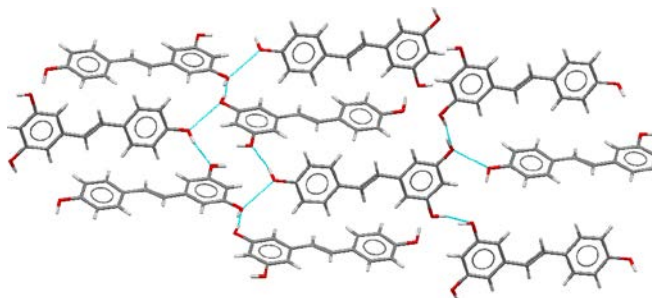
Figure 29. The structure of resveratrol (DALGON).[86]

The use of the planar pterostilbene molecule as a potential coformer in pharmaceutical cocrystallization is highlighted by the existence of five known cocrystals of pterostilbene with different APIs. Cocrystal formation in the case of the pterostilbene-piperazine (2:1) cocrystal is driven by two distinct phenol O-H$\cdots$N piperazine hydrogen bonded interactions between adjacent pterostilbene and piperazine molecules (OWAVUE) (Figure 30).[87]
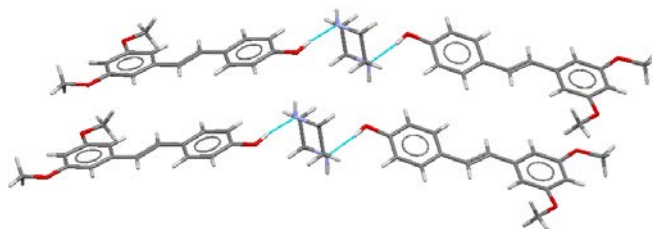

Figure 30. The structure of 2:1 pterostilbene-piperazine cocrystal (OWAVUE).[87]

The structure of pterostilbene-glutaric acid (1:1) cocrystal displays two interesting features (OWAWAL). First, one of the acid moiety of the dicarboxylic acid is forming an expected $R_2^2(8)$ acid-acid homodimer (Figure 31).[87] Second, the other acid moiety of two glutaric acid molecules coupled with the phenolic substituent of two adjacent pterostilbene molecules are forming a tetrameric acid-phenol-acid-phenol $R_4^4(12)$ supramolecular heterosynthon. There are 160 occurrences of this motif in the CSD.[39,40]
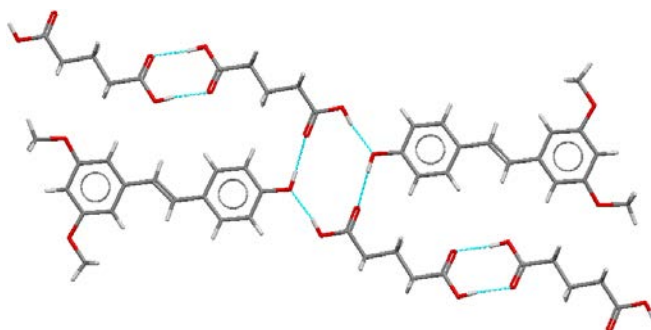
Figure 31. The structure of the pterostilbene-glutaric acid cocrystal (OWAWAL).[87]

The structure of two polymorphs of the pterostilbene-caffeine (1:1) cocrystals display the expected phenol O-H···O=C caffeine intermolecular interactions as pterostilbene is a single point hydrogen bond donor and caffeine is a hydrogen bond acceptor (YABHAM and YABHAM01) (Figure 32).[88] In comparison, the pterostilbene-carbamazepine (1:1) cocrystal displays the amide-amide homodimer for carbamazepine, where, in the absence of any other suitable hydrogen bond acceptors, the phenolic substituent of pterostilbene is satisfying the carbonyl groups of the amide-amide dimer on both ends *via* phenol O-H···O=C amide hydrogen bonds (YABHIU) (Figure 33).[88]
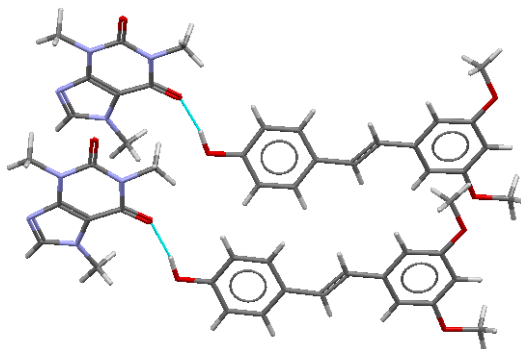

Figure 32. The structure of pterostilbene-caffeine (1:1) cocrystal (YABHAM).[88]
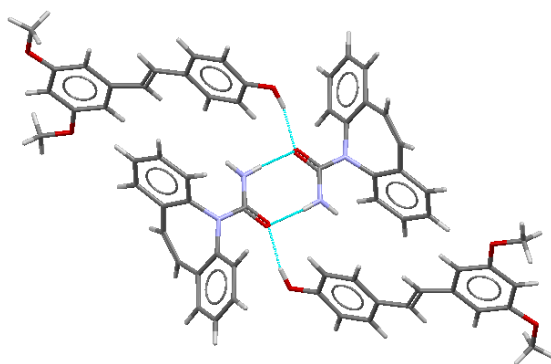
Figure 33. The structure of pterostilbene-carbamazepine (1:1) cocrystal (YABHIU).[88]

It is important to know the structural classification of flavonoids to gain a better understanding of the type and position of the hydrogen-bonded interactions observed in the structures. All flavonoids have a common C6-C3-C6 phenyl-benzopyran backbone, where the position of the phenyl ring relative to the benzopyran moiety allows for a clear distinction to be made between flavonoids (2-phenyl-benzopyrans), isoflavonoids (3-phenyl-benzopyrans) and neoflavonoids (4-phenyl-benzopyrans) (Figure 34).[89,90] These are further subdivided into groups based on the central ring oxidation and on the presence of hydroxyl groups. The most common flavonoids are flavonols (flavones with a 3-OH group), flavones (with a C2-C3 double bond and a C4-oxo functionality), and flavanones (with a C2-C3 single bond), whereas abundant isoflavonoids include isoflavones (the analogue of flavones).
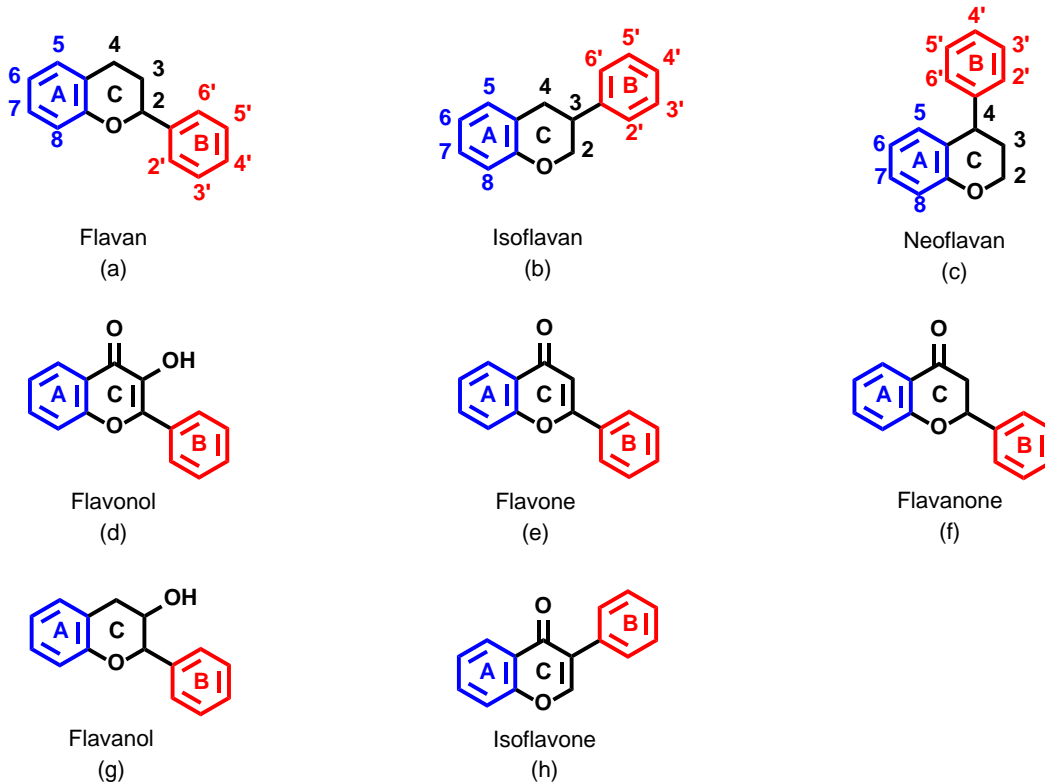
Figure 34. Structural backbone of the three main flavonoid groups: (a) flavan; (b) isoflavan; and (c) neoflavan. These can be classified into the common flavonoid classes: (d) flavonol; (e) flavone; (f) flavanone; (g) isoflavone; and (h) flavanol. Atom numbering and ring nomenclature are also included.

The 1:2 cocrystal of myricetin with triphenylphosphine oxide displays the expected intramolecular O-H···O=C hydrogen bond between the phenolic moiety on the benzene ring and the carbonyl on the pyrone ring (PILCIW) (Figure 35).[91] The phenolic substituents on ring B are forming two discrete phenol O-H···O=P hydrogen bonds which act as the driving force for cocrystal formation, whereas the phenolic substituent on ring A is hydrogen-bonded to the phenol moiety on ring B. Interestingly, the hydroxy substituent α to the carbonyl group on ring C is not involved in any structure defining hydrogen bonds.
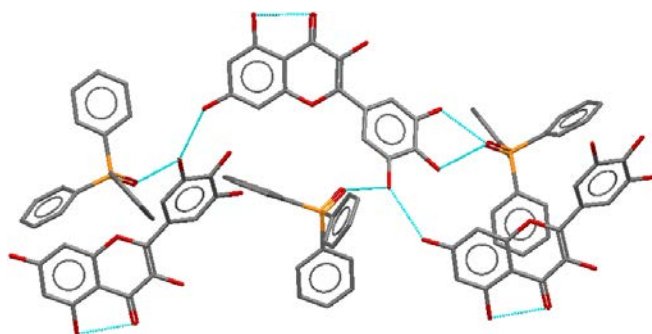
Figure 35. The structure of myricetin-triphenylphosphine oxide cocrystal (PILCIW).[91]

The structure of the 1:1 cocrystal of myricetin with the API piracetam reveals that the intramolecular hydrogen bond between substituents on ring A and C is retained, and cocrystal formation is accomplished by hydrogen bonds between ring B phenol O-H$\cdots$O=C amide and amide N-H$\cdots$O phenol (α to the carbonyl on pyrone ring, ring C) moieties resulting in a $R_2^2(12)$ molecular heterodimer (FIXROV) (Figure 36).[92] The heterodimers are extended into ribbons *via* ring B phenol O-H$\cdots$O=C cyclic carbonyl of piracetam and amide (second hydrogen atom) N-H$\cdots$O phenol (ring B) intermolecular interactions. The remaining phenolic substituents on myricetin help assemble the 3-D supramolecular architecture by phenol O-H$\cdots$O=C cyclic carbonyl of piracetam, phenol O-H$\cdots$O phenol and phenol O-H$\cdots$O=C amide hydrogen bonds.
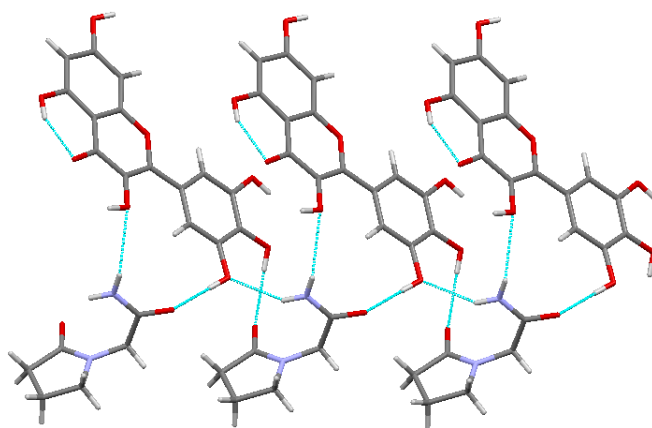

Figure 36. The structure of myricetin-piracetam cocrystal (FIXROV).[92]

There are eight known structures involving quercetin (see Table 1). The structure of quercetin monohydrate reveals four key features (AKIJEK) (Figure 37).[93] The first is an intramolecular O-H⋯O=C hydrogen bond between the phenolic moiety on ring A and the carbonyl group on ring C. Second, a dimer motif between adjacent quercetin molecules *via* O-H⋯O=C hydrogen bonds between the carbonyl group on ring C and the hydroxy group *α* to the carbonyl group is observed. Third, two of the phenolic substituents on ring A and B are forming orthogonal chains *via* phenol O-H⋯O phenol intermolecular hydrogen bonds. Last, the water molecule is interacting with the remaining phenolic substituent on ring B *via* phenol O-H⋯O water hydrogen bonds as well as with the carbonyl group on ring C, thus forming a bridge between two layers.
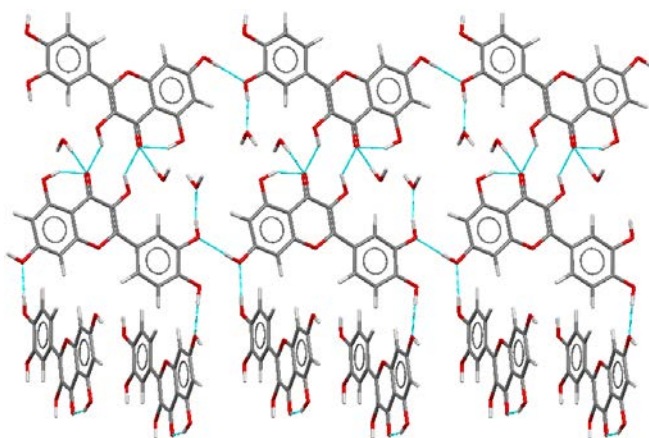
Figure 37. The structure of quercetin monohydrate (AKIJEK).[93]

Interestingly, in the structure of quercetin dihydrate the intramolecular hydrogen bond has been retained, whereas the dimer motif and the 1-D chain has given way to multiple water O-H⋯O phenol and phenol O-H⋯O water hydrogen bonds (FEFBEX01).[94] The 2:3 cocrystal of quercetin with 1,4-diazabicyclo[2.2.2]octane (DABCO) shows the expected intramolecular hydrogen bond as well as the hydrogen-bonded dimer motif between adjacent quercetin

molecules (COLHIV). The three remaining phenolic substituents on rings A and B are hydrogen bonding with the nitrogen atoms of three different DABCO molecules (Figure 38).[95]

Figure 38. The structure of quercetin-DABCO cocrystal (COLHIV).[95]
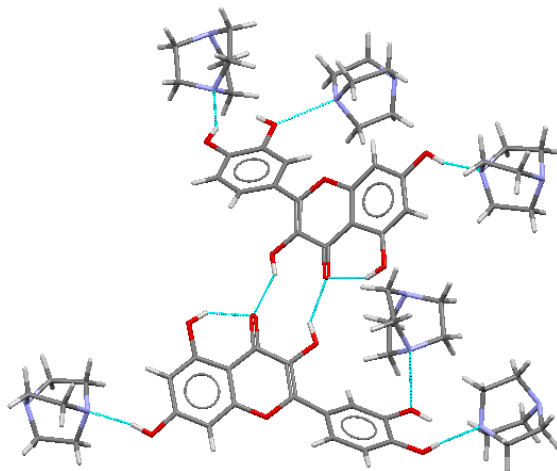
In comparison, the quercetin-isonicotinamide cocrystal retains only the expected intramolecular hydrogen bond, whereas the flavonoid dimer motif as observed in the quercetin-DABCO cocrystal is absent. The catechol end of quercetin (ring B) is forming a $R_2^2(10)$ supramolecular homodimer, while the dimer is flanked on either sides by two $R_3^3(8)$ dimers formed *via* phenol O-H···O=C amide and amide N-H···O phenol hydrogen bonds (Figure 39).[96] This four component supramolecular assembly between two quercetin and two isonicotinamide molecules can also be described by the $R_4^4(18)$ graph set. Furthermore, this assembly is extended into 1-D ribbons *via* ring A phenol O-H···N$_{arom}$ intermolecular interactions. Interestingly, the hydroxy substituent α to the carbonyl group on ring C of quercetin is not involved in any structure-defining hydrogen bonds, and the carbonyl group is capped by the *anti*-amide hydrogen atom. Multiple amide N-H···O=C quercetin hydrogen bonds are responsible for the generation of the 2-D layered architecture.
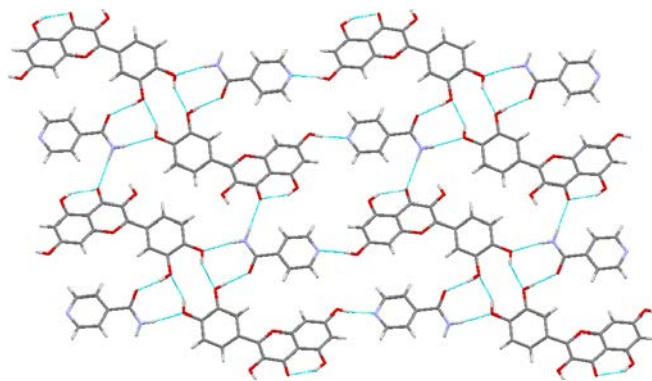
Figure 39. The structure of quercetin-isonicotinamide cocrystal.[96]

The structure of quercetin-theobromine (1:1) dihydrate retains the expected intramolecular hydrogen bond along with the dimer motif (MUPPOD) (Figure 40).[66] The amide moiety on theobromine is forming an $R_2^2(8)$ amide-amide homodimer, while adjacent quercetin dimers and theobromine dimers are interlinked *via* ring B phenol O-H···O=C theobromine, ring A phenol O-H···O water, and water O-H···N$_{arom}$ hydrogen bonds (water molecules act as bridges).
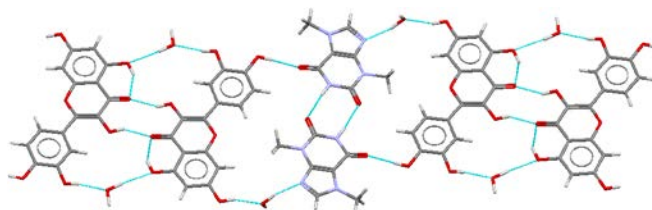
Figure 40. The structure of quercetin-theobromine dihydrate (MUPPOD).[66]

The fisetin-isonicotinamide (1:1) cocrystal has identical supramolecular motifs to that seen in the quercetin-isonicotinamide cocrystal, wherein the $R_2^2(10)$ catechol homodimer is flanked on either sides by two $R_3^3(8)$ phenol-amide heterodimers (ZIKNOY) (Figure 41).[97] Extended 2-D sheets are formed *via* multiple ring A phenol O-H···N$_{arom}$ and amide N-H···O=C carbonyl (ring C) hydrogen bonds. Interestingly, the difference (in terms of supramolecular synthons) between these cocrystals is the presence of the flavonoid dimer motif in the fisetin-

isonicotinamide cocrystal (extends the 2-D sheets into a 3-D architecture), which is clearly absent in the quercetin-isonicotinamide, even though an hydroxy group α to the carbonyl group exists on the quercetin backbone. In contrast, the $R_2^2(10)$ catechol homodimer flanked by the $R_3^3(8)$ phenol-amide heterodimer motif is absent in fisetin-nicotinamide (1:2) ethanol hemisolvate (ZIKPAM) (Figure 42).[97] The flavonoid dimer motif is retained and the supramolecular architecture is assembled *via* ring B phenol O-H···N_{arom}, ring A phenol O-H···O=C nicotinamide, amide N-H···O=C amide [amide C(4) chain], and amide N-H···O phenol (ring A) hydrogen bonds.
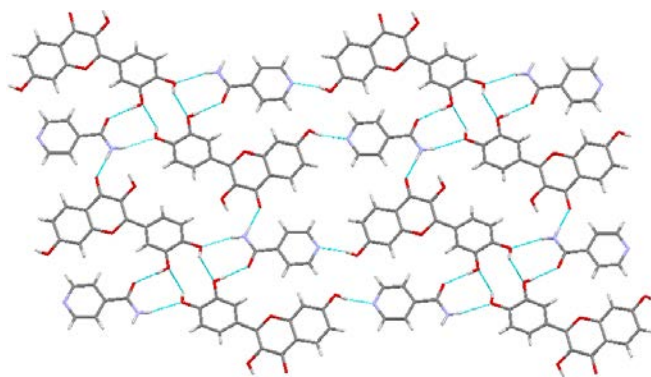

Figure 41. The structure of fisetin-isonicotinamide cocrystal (ZIKNOY).[97]
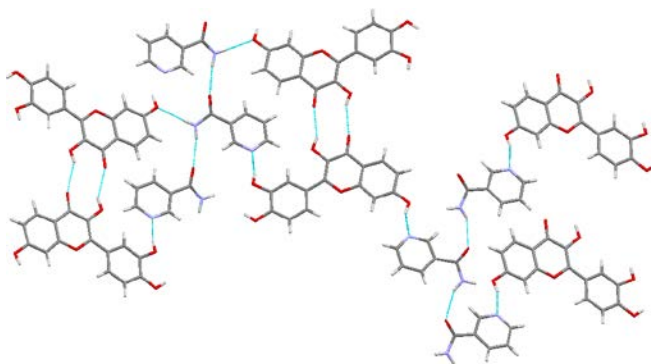

Figure 42. The structure of fisetin-nicotinamide ethanol hemisolvate (ZIKPAM).[97]

An examination of the structure of luteolin hemihydrate reveals three key features (OJEQUP) (Figure 43).[98] First, the intramolecular hydrogen bond between the phenolic substituent (ring A) and the carbonyl group (ring C), as observed in flavonoids **11**-**12**, **14-18**, persists. Second, in the absence of the hydroxy substituent α to the carbonyl group on ring C (with the result that dimer formation is not feasible) an intermolecular O-H···O=C hydrogen bond between adjacent luteolin molecules is observed. Third, the remaining phenolic substituents on ring A and B form multiple phenol O-H···O phenol hydrogen bonds, thus extending the supramolecular architecture.
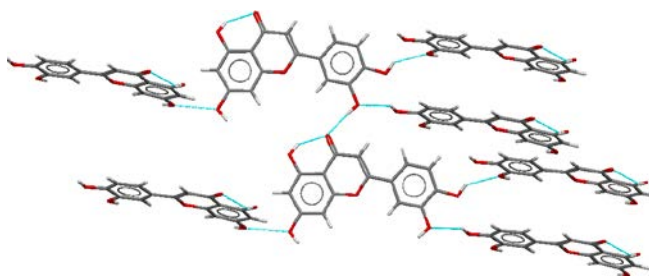
Figure 43. The structure of luteolin hemihydrate (OJEQUP).[98]

Although polymorphic cocrystals of APIs are not uncommon,[88,99,100] the first report of flavonoid polymorphic cocrystals was by Sowa *et al.*,[97] wherein two polymorphs of 1:1 luteolin-isonicotinamide cocrystal were observed. Form I has an identical crystal structure to the quercetin-isonicotinamide and fisetin-isonicotinamide cocrystals, wherein the $R_2^2(10)$ catechol homodimer is flanked on either sides by two $R_3^3(8)$ phenol-amide heterodimers (ZIKPUG) (Figure 44).[97] Furthermore, the extended 2-D sheet like architecture is formed *via* multiple ring A phenol O-H···N$_{arom}$ and amide N-H···O=C carbonyl (ring C) intermolecular hydrogen bonds. In contrast, Form II does not form the catechol homodimer motif in the solid-state, and instead cocrystal formation is driven by ring A phenol O-H···N$_{arom}$, amide N-H···O phenol (ring A), and

ring B phenol O-H···O=C amide hydrogen bonds (ZIKPUG02) (Figure 45). Also, the carbonyl substituent on ring C is satisfied by the phenolic substituent of an adjacent luteolin molecule.[97]
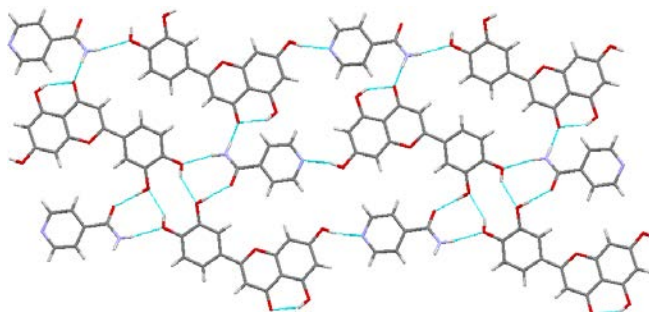
Figure 44. The structure of luteolin-isonicotinamide cocrystal (Form I) (ZIKPUG).[97]
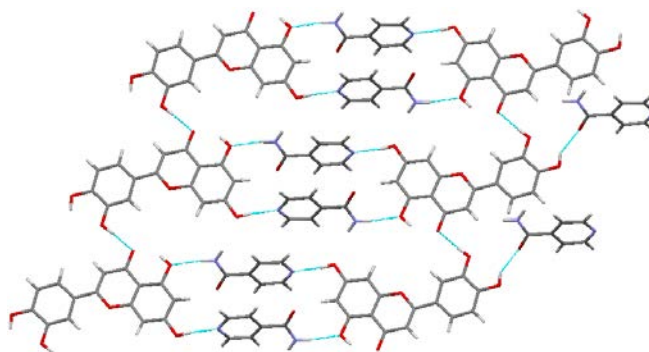
Figure 45. The structure of luteolin-isonicotinamide cocrystal (Form II) (ZIKPUG02).[97]

There are two known structures involving baicalein (Table 1). The structure of baicalein reveals three key features (RAMGOB01) (Figure 46).[101] The first is the expected intramolecular O-H···O=C hydrogen bond. Second, a $R_2^2(10)$ catechol homodimer motif (ring A) between adjacent baicalein molecules *via* O-H···O hydrogen bonds is observed. Third, in the absence of the hydroxy substituent α to the carbonyl group on ring C (with the result that dimer formation is not feasible) an intermolecular O-H···O=C hydrogen bond between adjacent baicalein molecules is observed.
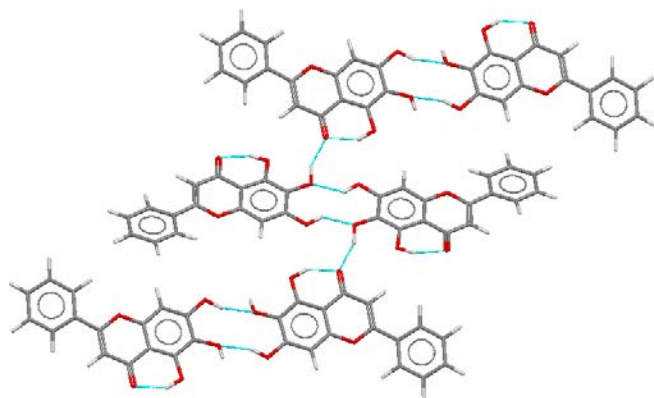
Figure 46. The structure of baicalein (RAMGOB01).[101]

An examination of the crystal structure of 1:1 baicalein-nicotinamide cocrystal shows the intramolecular hydrogen bond between the phenolic moiety on ring A and the carbonyl group on ring C being retained (GAZWUB) (Figure 47).[102] Interestingly, the $R_2^2(10)$ catechol homodimer observed in the structure of baicalein has given way to the $R_2^2(9)$ heterodimer motif formed between the catechol moiety on ring A and the amide group of nicotinamide *via* phenol O-H···O=C amide and amide N-H···O phenol hydrogen bonds. Also, the *exo* phenolic hydrogen atom of the catechol-amide dimer motif is hydrogen-bonded to N_{arom} nicotinamide. Furthermore, the architecture is extended *via* N-H···O=C intermolecular amide C(4) chains.

Figure 47. The structure of baicalein-nicotinamide cocrystal (GAZWUB).[102]

To date the only known crystal structure of naringenin is the structure itself, which displays an expected intramolecular ring A phenol O-H···O=C carbonyl (ring C) hydrogen bond

(DOLRIF). The phenolic substituents on rings A and B from two adjacent naringenin molecules upon hydrogen bonding form a unique $R_2^2(24)$ supramolecular homosynthon. In the absence of the hydroxy substituent α to the carbonyl group 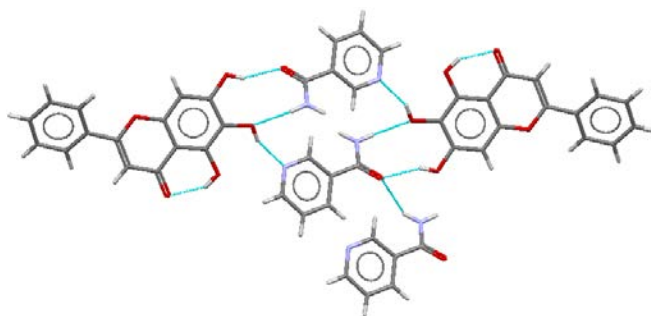on ring C, the remaining phenolic substituent on ring B caps the carbonyl group, thus extending the homosynthons into 1-D ribbons (Figure 48).[103]
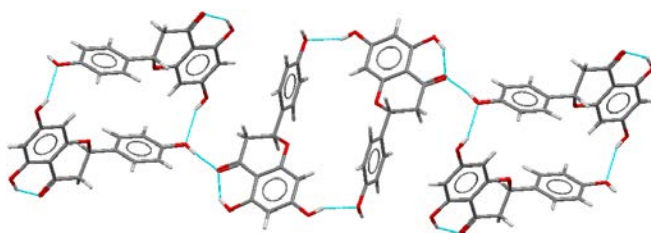
Figure 48. The structure of naringenin (DOLRIF).[103]

There are four known structures involving hesperetin (see Table 1). Anhydrous hesperetin displays common structure defining hydrogen bonds to those seen in luteolin hemihydrate and naringenin, wherein the expected intramolecular (O-H⋯O=C) hydrogen bond along with the phenolic substituent on ring A being hydrogen-bonded to the carbonyl group on ring C (flavonoid capping motif) is observed, which leads to the formation of 1-D chains (YEHROS) (Figure 49 a).[104] Similarly, in the structure of hesperetin monohydrate the expected intramolecular and intermolecular phenol O-H⋯O=C carbonyl hydrogen bonds have been retained leading to the formation of 1-D chains (FOYTOC) (Figure 49 b).[105] Furthermore, the water molecules act as a bridge between two adjacent 1-D chains *via* ring A phenol O-H⋯O water and water O-H⋯O phenol (ring B) hydrogen bonds. The hydroxy substituent α to the methoxy group on ring B in hesperetin monohydrate is involved in hydrogen bonding, in contrast to the anhydrous hesperetin.
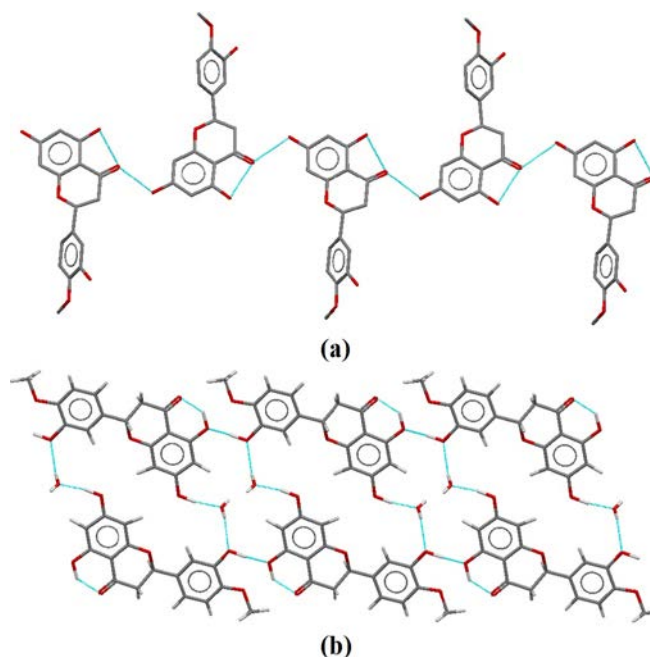
Figure 49. The structure of: **(a)** hesperetin (YEHROS);[104] and **(b)** hesperetin monohydrate (FOYTOC).[105]

In the structure of genistein a combination of two phenol O-H⋯O phenol (between substituents on rings A and B) and two ring A phenol O-H⋯O=C carbonyl (ring C) (flavonoid capping motif) hydrogen bonds between four adjacent genistein molecules leads to the formation of a $R_4^4(42)$ supramolecular motif, which are interconnected by a $R_4^4(22)$ motif (GENIST) (Figure 50).[106]
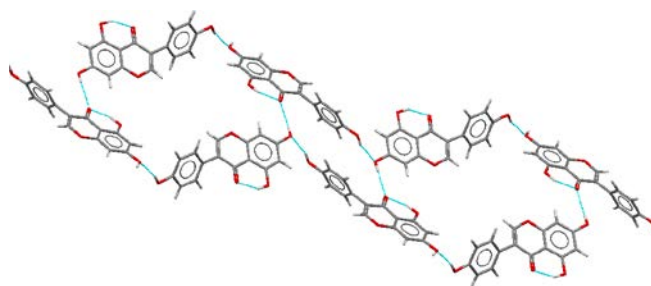
Figure 50. The structure of genistein (GENIST).[106]

The genistein-isonicotinamide (1:2) cocrystal retains the intramolecular hydrogen bonds, whereas the intermolecular flavonoid capping motif is absent (YIKRAN) (Figure 51).[107] The amide-amide homodimers are interconnected by discrete phenol O-H···N_{arom} hydrogen bonds leading to the formation of 1-D chains. Additionally, an extended architecture is formed *via anti*-amide N-H···O phenol (rings A and B) intermolecular interactions. In contrast, the amide-amide dimer is absent in genistein-nicotinamide (1:1) monohydrate, and has been replaced by amide N-H···O phenol (ring B) hydrogen bonds (ZIKPIU). Furthermore, ring A phenol O-H···N_{arom} intermolecular interactions lead to the formation of 1-D chains (Figure 52).[97] The remaining phenolic substituent on ring B is hydrogen-bonded to a water molecule (which is a reflection of the reduced stoichiometry of the coformer), and the 3-D supramolecular architecture is assembled *via* water O-H···O=C amide and water O-H···O phenol hydrogen bonds.
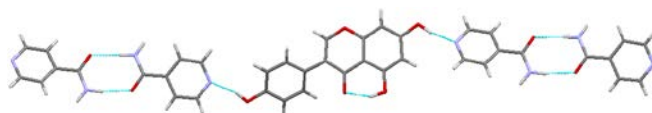
Figure 51. The structure of genistein-isonicotinamide cocrystal (YIKRAN).[107]
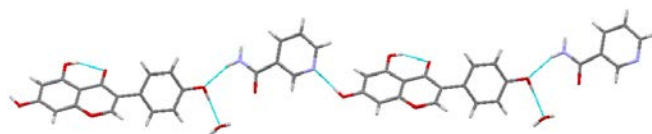
Figure 52. The structure of genistein-nicotinamide monohydrate (ZIKPIU).[97]

The diasteriomeric flavanols (+)-(2*R*,3*S*)-catechin and (-)-(2*R*,3*R*)-epicatechin are the naturally occurring forms and are also commonly found functionalized as the gallate ester. An important feature of the structure of epicatechin is the $R_4^4(8)$ hydroxy tetramer formed *via* O-H···O hydrogen-bonded interactions between three phenolic moieties (rings A and B) and one

hydroxy substituent (ring C) on epicatechin (COWHUR) (Figure 53).[108] The remaining phenolic substituent on ring B is hydrogen bonded to the oxygen atom of ring C. In comparison, the only stable hydrate seen for catechin (4.5) is the one in which three of the hydroxy substituents interact with water molecules, whereas the remaining two hydroxy substituents are involved in phenol O-H⋯O phenol hydrogen bonds (LUXWOR).[109] Cocrystal formation in epicatechin-caffeine dihydrate (WUSFIA)[110] and catechin-caffeine trihydrate (OZIDUX)[111] molecular complexes is achieved *via* ring A hydroxy O-H⋯O=C caffeine hydrogen bonds, whereas all other hydrogen bond donors and acceptors on catechin and the coformer caffeine are satisfied by the water molecules *via* multiple O-H⋯O hydrogen bonds (Figure 54).
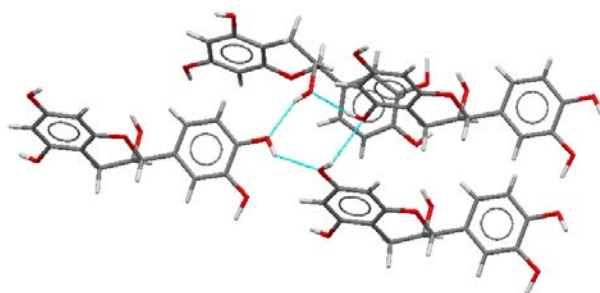
Figure 53. The structure of epicatechin (COWHUR).[108]
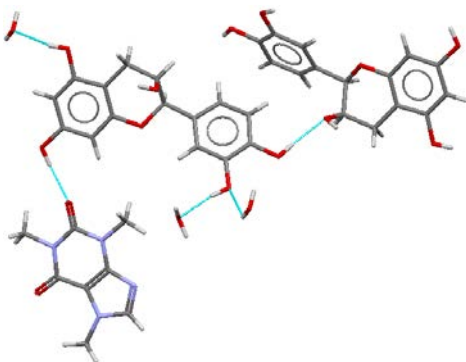
Figure 54. The structure of epicatechin-caffeine dihydrate (WUSFIA).[110]

There are two known hydrated molecular complexes of catechin gallate with caffeine. The first is the 1:2:4 catechin gallate:caffeine:water molecular complex, wherein the expected motif (phenol O-H···N$_{arom}$) is not observed (OZIDIL). Instead cocrystal formation is accomplished *via* rings A and B phenol O-H···O=C caffeine hydrogen bonds, whereas the water molecules are interacting with all the hydrogen bond donor/acceptor sites on both catechin gallate and caffeine molecules (Figure 55).[111] In comparison, the 2:4:6 epicatechin gallate:caffeine:water molecular complex displays the expected ring B phenol O-H···N$_{arom}$ and ring A phenol O-H···O=C caffeine intermolecular interactions (WUSFOG) (Figure 56).[110] Also, π-π interactions are prevalent in this supramolecular architecture. The water molecules are satisfying the remaining hydrogen bond donors/acceptors in the system.
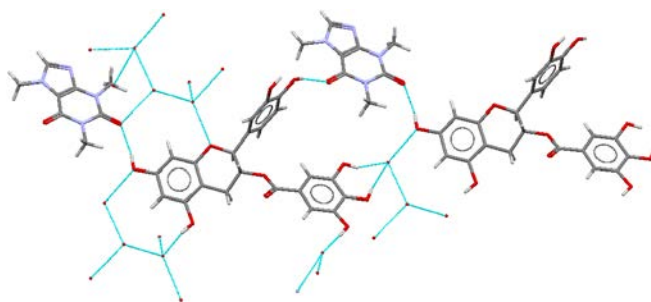
Figure 55. The structure of catechin gallate:caffeine:water (1:2:4) molecular complex (OZIDIL).[111]
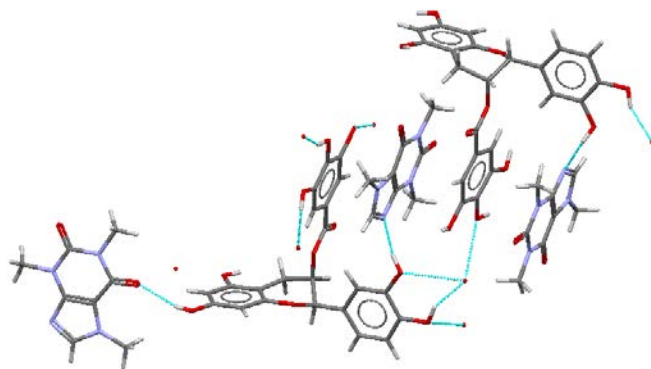
Figure 56. The structure of epicatechin gallate:caffeine:water (2:4:6) molecular complex (WUSFOG).[110]

There are twelve structures involving epigallocatechin gallate (EGCG) (see Table 1). Focussing initially on the structure of EGCG by itself, there are multiple characteristic phenol O-H···O phenol hydrogen bonds (Figure 57).[112] Similarly, EGCG monohydrate also displays multiple phenol O-H···O phenol hydrogen bonds, wherein one of the phenolic substituent is hydrogen-bonded to a water molecule, while another is hydrogen bonding with the carbonyl of the ester functional group (BONKOF) (Figure 58).[113]
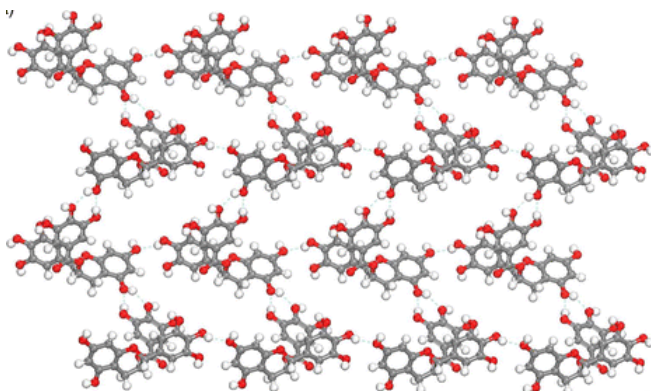
Figure 57. The structure of epigallocatechin gallate.[112]
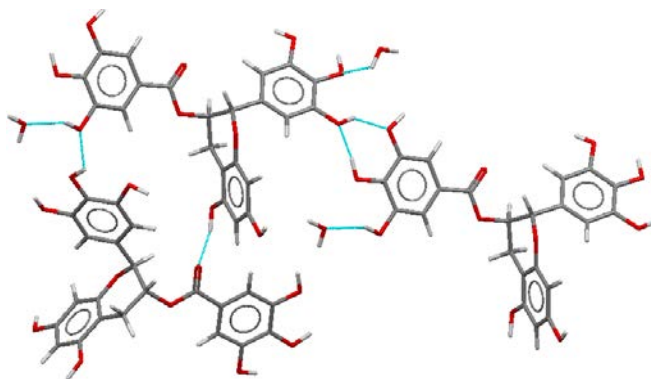
Figure 58. The structure of epigallocatechin gallate monohydrate (BONKOF).[113]

Epigallocatechin gallate (EGCG) has seven hydrated cocrystals, the most seen for any of the flavonoids. This can be a direct consequence of the presence of multiple hydroxy substituents on EGCG when compared to the other flavonoids. Of the three known hydrated cocrystals of EGCG with caffeine [trihydrate (RUNDUA),[114] hexahydrate (BONKIZ)[113] and heptahydrate (VEQTES)[115]], the trihydrate and hexahydrate display the expected ring B phenol O-H···N_{arom} and ring A phenol O-H···O=C caffeine motifs, where the water molecules are interacting with the remaining hydrogen bond donors/acceptors on EGCG and caffeine molecules (Figure 59). In the case of the heptahydrate complex, although the expected ring B phenol O-H···N_{arom} hydrogen-bonded interactions are observed, phenol O-H···O=C caffeine interactions have been displaced by water O-H···O=C caffeine hydrogen bonds, and water molecules are satisfying the remaining hydrogen bond donors and acceptors in the system (Figure 60).[115]
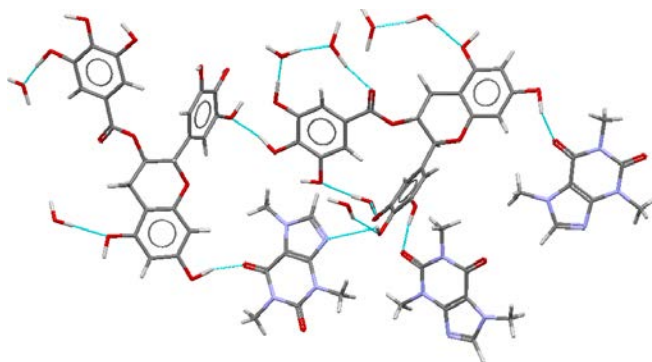
Figure 59. The structure of EGCG:caffeine:water (1:2:3) molecular complex (RUNDUA).[114]
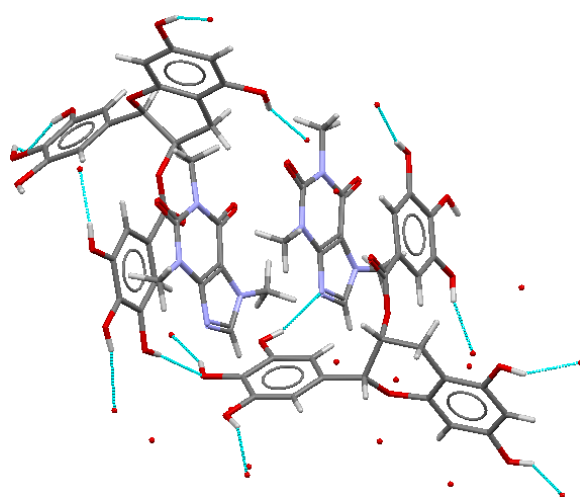
Figure 60. The structure of EGCG:caffeine:water (1:1:7) molecular complex (VEQTES).[115]

In both the hydrated cocrystals of EGCG with nicotinamide (1:1) [pentahydrate (VEQTIW)[115] and nonahydrate[112]], cocrystal formation is driven *via* expected phenol O-H···N$_{arom}$, phenol O-H···O=C nicotinamide, and nicotinamide N-H···O phenol hydrogen bonds, where the water molecules are satisfying the remaining hydrogen bond donors and acceptors (Figure 61). The structure of 1:1 EGCG-isonicotinamide pentahydrate has the same hydrogen bonded motifs as found in the hydrated EGCG-nicotinamide cocrystals (Figure 62).[112]
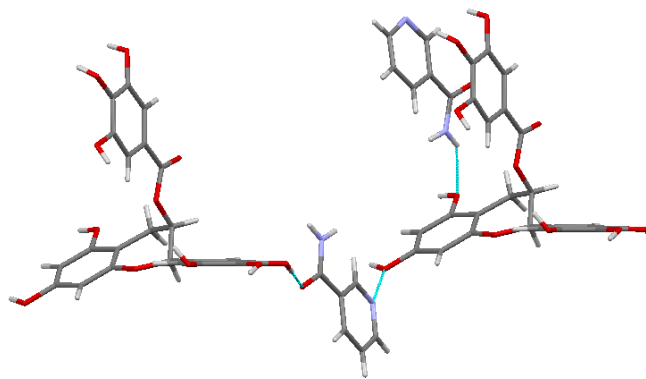
Figure 61. The structure of EGCG-nicotinamide (1:1) nonahydrate.[112]
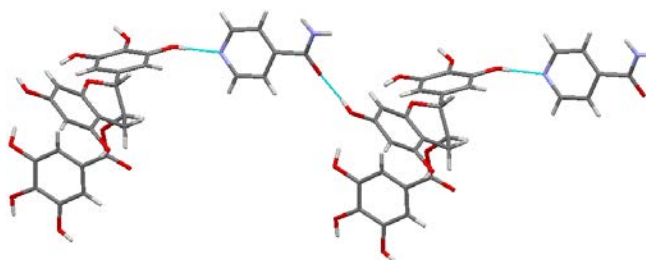
Figure 62. The structure of EGCG-isonicotinamide (1:1) pentahydrate.[112]

The structures of both racemic (NELRUR) and non-racemic forms (FAFXUF) of pinoresinol display similar supramolecular motifs, *i.e.* phenol O-H$\cdots$O phenol and phenol O-H$\cdots$O cyclic hydrogen bonds.[116,117] Despite having the same kinds of intermolecular interactions, the two structures are very different from each other. (+)-Pinoresinol displays orthogonal chains (Figure 63),[116] whereas the structure of racemic pinoresinol resembles a 2-D sheet (Figure 64).[117]
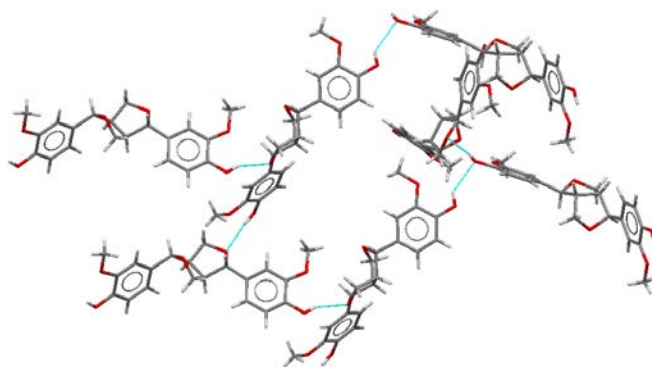
Figure 63. The structure of (+)-pinoresinol (FAFXUF).[116]
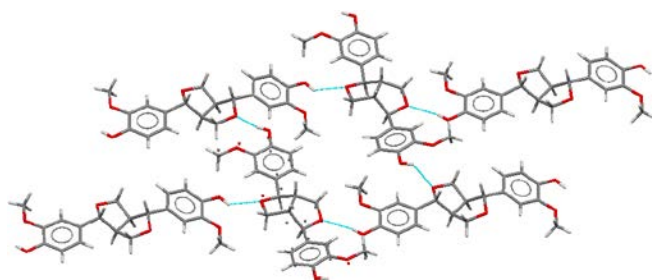
Figure 64. The structure of racemic pinoresinol (NELRUR).[117]

There are five known structures involving podophyllotoxin (see Table 1) which by itself exists as two forms. The first one does not display any discernible hydrogen bonds or short contacts (PACSUH).[118] However, the second form shows infinite 1-D chains formed *via* head-to-tail alcohol O-H···O methoxy hydrogen-bonded interactions (PACSUJ) (Figure 65).[119]
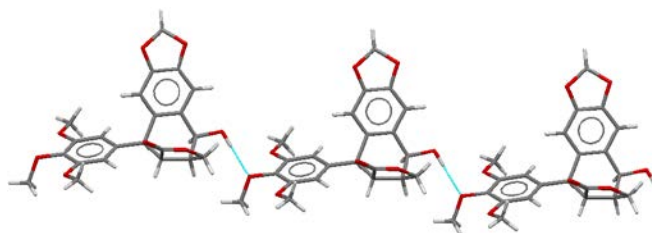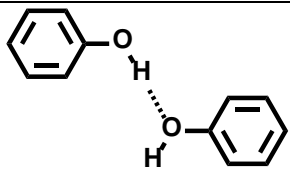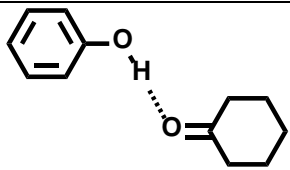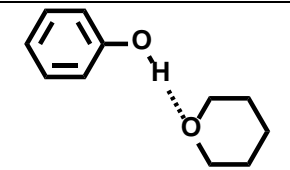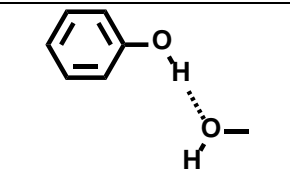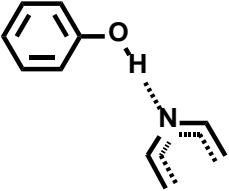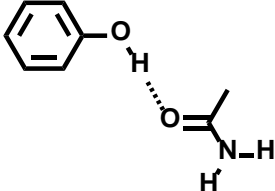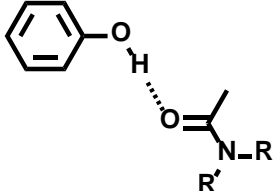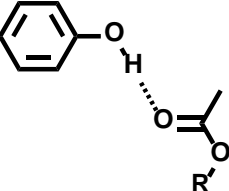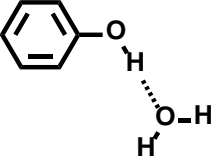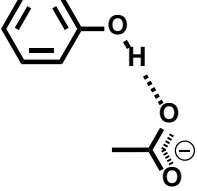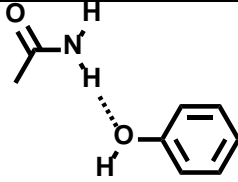
Figure 65. The structure of podophyllotoxin (PACSUJ).[119]
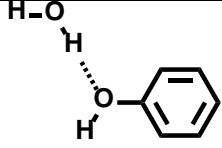
2.2.1 Common features observed for polyphenols

Some common structural features that are observed in the structures of different polyphenols including coumarin (**8**), stilbenes (**9**-**10**), flavonoids (**11**-**21**) and lignans (**22**-**23**) along with the robust intermolecular interactions, Table 3, which are present in these crystal structures are outlined in this section.

Table 3. The most common intra- and intermolecular interactions observed in the polyphenols have been organized in two categories: (i) phenols as donors; and (ii) phenols as acceptors.

Type of Interaction	Structure	Hydrated structures	Cocrystals	Hydrated cocrystals	Salts	Solvates
Phenols as donors						
	9, **15**, **16**, **18**, **19**, **21**, **22**	**12**, **14**, **17**, **19**, **21**	**11**(2), **12**, **13**, **14**	**19**, **21**(3)	**17**(2)	**12**(2), **21**
	15, **16**, **17**, **18**	**12**(2), **14**, **17**	**11**(2), **12**(2), **14**(2), **17**, **18**	**12**, **18**, **19**(2), **20**(2), **21**	**12**, **17**(2)	**12**(2), **13**
	11(2), **19**					**19**(2), **22**(2)
	19	**19**		**19**		**12**, **19**(2)

50

phenol O–H···N (pyrrolidine)			**12, 13, 14**(2)**, 15, 17, 18**	**18, 20, 21**(6)		**12**(2)**, 13, 19**
phenol O–H···O=C–NH₂			**10, 11, 12, 13, 14**(2)**, 15**	**21**(3)		**13**
phenol O–H···O=C–N(R)R′			**11**	**19**(2)**, 20**(2)**, 21**(2)		**12**
phenol O–H···O=C–OR′		**21**		**20**(2)**, 21**(2)		**21**
phenol O–H···O(H)–H (water)		**12**(2)**, 17, 19, 21**		**12, 18, 19**(2)**, 20**(2)**, 21**(5)	**12**	**21**
phenol O–H···carboxylate					**9, 12, 17**(2)**, 21**	
Phenols as acceptors						
amide N–H···O phenol			**11, 12, 13, 14**(2)**, 15, 17, 18**	**18, 21**(2)		**13**

		12(2), 17, 19, 21		12, 18, 19(2), 20(2), 21(5)	9, 12	21

Numbers in brackets indicate the number of times the particular interaction is observed in the appropriate compound (as identified in Figure 3).

In the absence of any competing hydrogen bond donors and acceptors the primary intermolecular interaction observed in the structures of polyphenols with no carboxylic acid moieties is phenol O-H$\cdots$O phenol hydrogen bonds (Table 3).[75] Upon cocrystallization, the observed motifs for the phenolic moieties, such as phenol O-H$\cdots$N$_{arom}$, phenol O-H$\cdots$O=C amide, and amide N-H$\cdots$O phenol, are representative of the coformer used and the functional groups present in the coformers.

The calculated MEPs of the polyphenols reinforces the observations made based on the existing single crystal data that phenols can act as effective hydrogen bond donors (Figure 66). Also, it allows for a closer examination of the hydrogen bonding capability of the phenolic substituents on rings A and B of the flavonoids. There is a ΔE difference of 3-18 kJ mol^{-1} between the best hydrogen bond donor on ring A and B for most of the flavonoids (**11**-**13**, **16**-**18**, **20**-**21**), which suggests that there is no real selectivity in hydrogen bonds between the two rings, and cocrystallization can occur *via* either end of the molecule. In the majority of cases with flavonoids cocrystal formation is driven *via* hydrogen bonds involving the phenolic groups on either one or both A and B rings with the coformer. This is even seen for luteolin (**14**) which has a large ΔE difference of 58 kJ mol^{-1}.

8 9 10 11

12 13 14

15 16 17

18 19 20

21 22 23
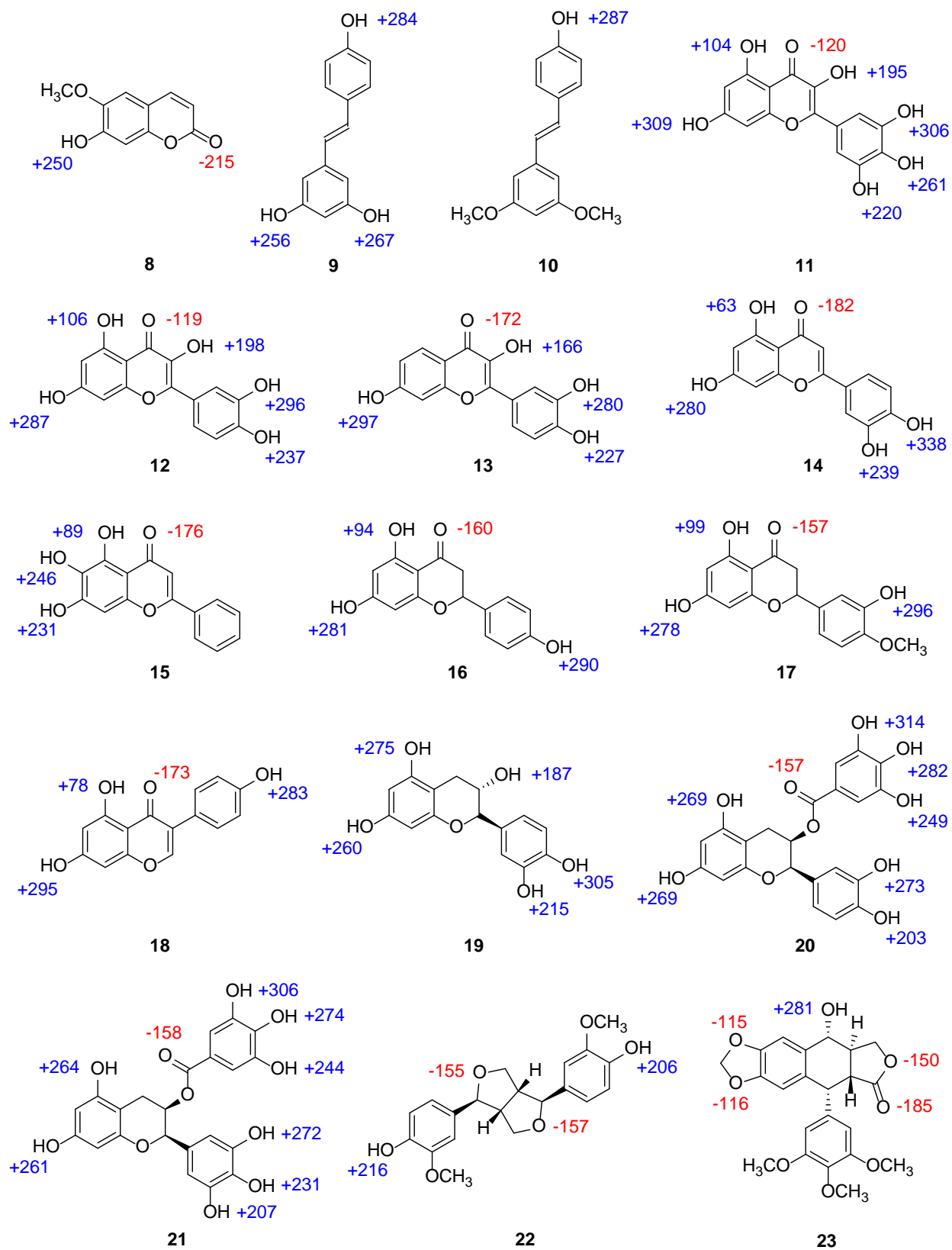
Figure 66. Calculated molecular electrostatic potentials (kJ mol^{-1}) for the polyphenols. Blue = positive potential, red = negative potential.

Flavonoids with the hydroxy group α to the carbonyl substituent on ring C (**11**-**13**) have a tendency to form a $R_2^2(10)$ flavonoid dimer motif (Figure 67 a), as has been commonly observed in the myriad of structures containing quercetin (**12**) and fisetin (**13**). Myricetin (**11**) is an exception to this since both its cocrystals do not exhibit this dimer motif. In contrast, in **14**-**17** the absence of the hydroxy group α to the carbonyl substituent on ring C means the dimer motif cannot be formed and instead the carbonyl substituent is usually capped by the phenolic substituent of an adjacent flavonoid molecule (Figure 67 b). This motif is commonly observed in the structures containing luteolin (**14**), baicalein (**15**), naringenin (**16**), and hesperetin (**17**), the exceptions being the cocrystal of baicalein with nicotinamide and the two salts of hesperetin with zwitterionic nicotinic and isonicotinic acids.
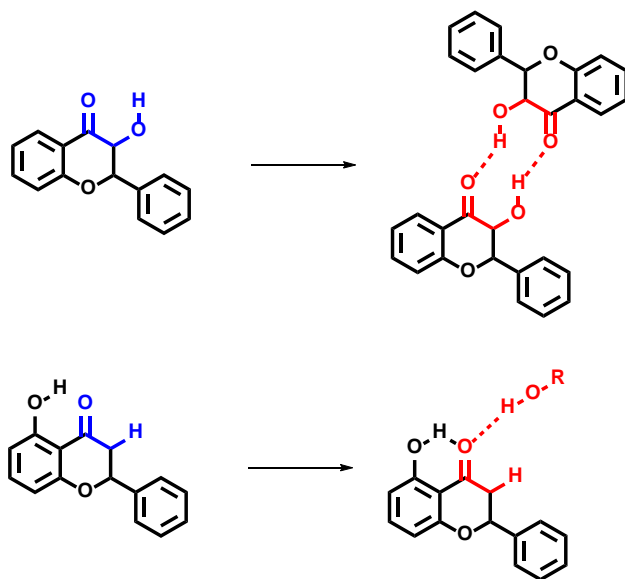
Figure 67. Common hydrogen-bonded motifs observed in flavonoids: flavonoid dimer motif (top) and flavonoid capping motif (bottom).

Another common structural feature observed in the isonicotinamide cocrystals of flavonoids with a catechol moiety on the ring B backbone (quercetin, fisetin, and luteolin), is the formation of the $R_2^2(10)$ supramolecular catechol homodimer, where the dimer is flanked on both sides by two $R_3^3(8)$ phenol-amide heterodimers formed *via* phenol O-H$\cdots$O=C amide and amide N-H$\cdots$O phenol hydrogen bonds (Figure 68). This four component supramolecular assembly between two catechol moieties and two isonicotinamide molecules can also be described by the $R_4^4(18)$ graph set.
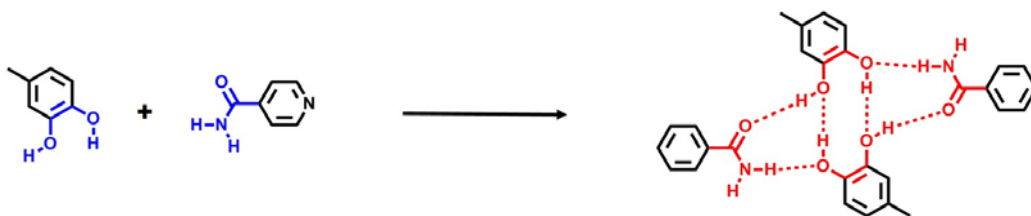
Figure 68. The 'flanked dimer' motif commonly observed in the isonicotinamide cocrystals of flavonoids containing the catechol moiety.

Knowledge of the structural chemistry of hydrates of organic molecules can provide insight into the tendency of these molecules to form cocrystals.[120-122] There have been a variety of theories postulated to explain hydrate formation for organic molecules. Thus, hydrates are more likely to form for: (a) a low hydrogen bond donor/hydrogen bond acceptor ratio;[123] (b) charged compounds;[124] (c) multiple counts of a functional group;[124] (d) high molecular weight compounds;[125] and (e) spatial constraints in hydrogen bonding.[125] In addition, the role of hydrates in crystal engineering have been recently examined for a wide variety of supramolecular synthons.[66] Analysis of the available single crystal data for phenolic acids (**1**-**7**) and polyphenols (**8**-**23**) indicates that further structural data are required to rationalize which hydrate formation theories apply for these classes of compounds.

3. Vitamins

Vitamins are essential organic compounds that are required by the human body as they are not produced by humans in sufficient quantities.[126] They are essential for metabolism and are usually obtained from natural sources.[127] Although they are readily available over the counter and are easily patentable,[126,127] they have not been extensively used as coformers in cocrystallization. A synergistic approach to cocrystallization of vitamins with other APIs can not only help improve the physicochemical properties of APIs, but also tap into the possibility of developing dual drugs with multiple benefits. Eleven different molecules have been explored in this category, of which two are vitamin A (**24**-**25**), five vitamin B (**26**-**29**, **33**), one vitamin C (**30**), two vitamin D (**31**-**32**), and one vitamin K (**34**) (Figure 4). Nicotinamide and nicotinic acid (vitamin B$_3$ and derivative) have been extensively used in cocrystallization and their structural chemistry reviewed.[128]

Focusing initially on the aldehyde containing molecule retinal, there are five distinct solid state structures of retinal known, differing in the *cis*/*trans* conformations at the multiple alkene moieties. Of the five stereoisomers, four have no discernible hydrogen bonds in the architecture and are governed by weak C-H$\cdots$O=C aldehyde intermolecular interactions (CRETAL01, CRETAL10, RETNLA10 and TRETAL01),[129-132] although in one case, the supramolecular architecture is assembled *via* aldehyde C-H$\cdots$O=C aldehyde hydrogen-bonded homodimer motif (FAHNEH) (Figure 69).[133] These interactions are not uncommon as there are over 200 reported examples in the CSD of the aldehyde-aldehyde homodimer.[39,40]
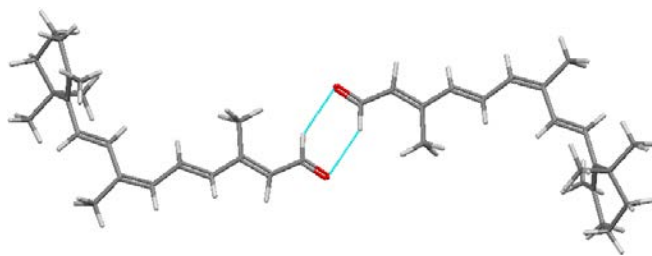
Figure 69. The structure of 9-*cis*-retinal (FAHNEH).[133]

The carboxylic acid derivative of vitamin A is retinoic acid and there are three isomers of the structure of retinoic acid (TUDSIU, VITAAC01 and VITAAC10),[134,135] which can again be attributed to the presence of differing *cis*/*trans* conformations at the multiple alkene moieties. All isomers display an expected acid-acid homodimer *via* O-H⋯O=C hydrogen-bonded interactions (Figure 70).[135] The all *trans*-isomer has been crystallized with the plasma protein transthyretin.[136]
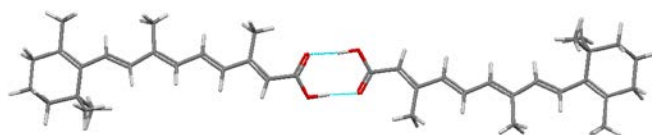
Figure 70. The structure of retinoic acid (VITAAC01).[135]

Riboflavin (vitamin B_2) is a molecule that combines hydroxy functional groups with nitrogen containing heterocyclic rings and therefore is capable of very diverse hydrogen-bonded interactions. The structure of 1:1 riboflavin-adenine trihydrate (ADRBFT10) reveals that supramolecular assembly occurs *via* three key intermolecular interactions: (a) riboflavin N-H⋯N adenine; (b) adenine N-H⋯O=C riboflavin; and (c) adenine N-H⋯N riboflavin hydrogen bonds, all of which involve imidazole (Figure 71).[137] These interactions between riboflavin and adenine molecules resemble a Hoogsteen base pair.[138] The water molecules and the hydroxy substituents on riboflavin interact within themselves to complete the hydrogen-bonded extended network.
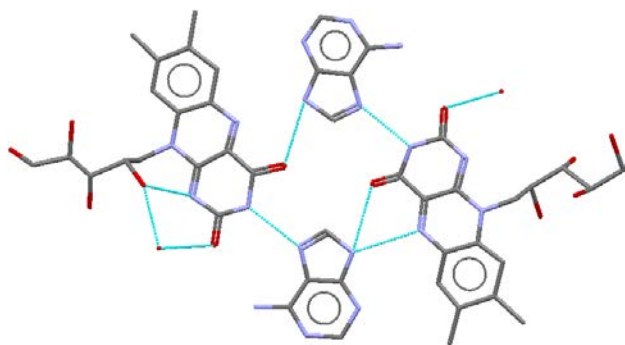
Figure 71. The structure of 1:1 riboflavin-adenine trihydrate (ADRBFT10).[137]

The hydrogen-bonded network in 1:1 riboflavin-5'-bromo-5'-deoxyadenosine trihydrate (RIBBAD) is similar to that observed in riboflavin-adenine trihydrate. Hoogsteen base pair[138] formation takes place *via* two intermolecular interactions: (a) deoxyadenosine N-H···O=C riboflavin; and (b) riboflavin N-H···N deoxyadenosine (imidazole) (Figure 72).[139] Other key hydrogen bonds include deoxyadenosine N-H···O riboflavin (alcohol) and deoxyadenosine (alcohol) O-H···O=C riboflavin, in which water molecules are hydrogen-bonded with the remaining donors and acceptors.
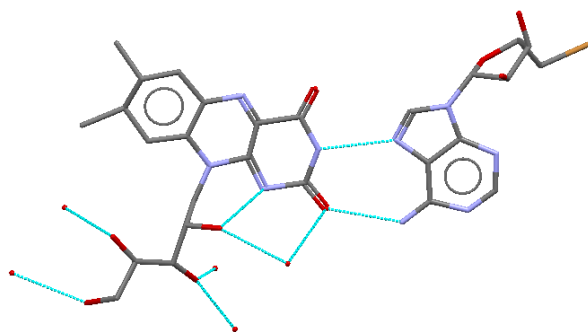
Figure 72. The structure of 1:1 riboflavin-5'-bromo-5'-deoxyadenosine trihydrate (RIBBAD).[139]

There is only one structure reported to date for pantothenic acid which is with the zwitterionic amino acid *L*-lysine (BACWUX10),[140] and a wide diversity of intermolecular interactions are observed in this architecture.

Pyridoxine (vitamin B_6) consists of the hydroxy and the pyridyl functional groups, hence it is capable of acting as both a hydrogen bond donor and acceptor. Anhydrous pyridoxine displays an infinite 1-D chain formed by head-to-tail hydrogen-bonded interactions between the pyridyl nitrogen atom and the hydroxy group in the *para* position (BITZAF) (Figure 73).[141] An extended architecture is formed *via meta* position hydroxy groups hydrogen bonding with each other, whereas the remaining phenolic substituent is hydrogen-bonded in an intramolecular fashion to the *para*-hydroxyl group.
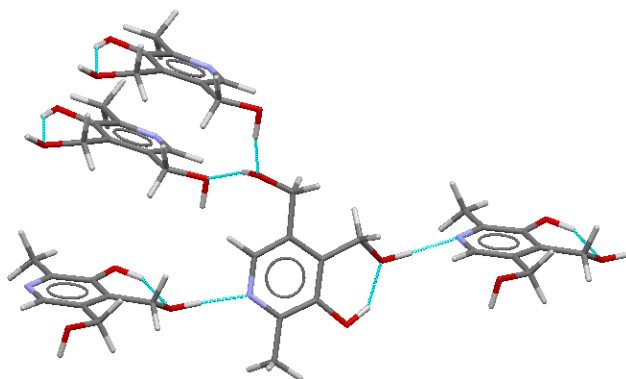
Figure 73. The structure of pyridoxine (BITZAF).[141]

Cocrystallizing pyridoxine with a strong hydrogen bond donor such as picric acid (1:1) leads to complete proton transfer from picric acid to the pyridyl nitrogen atom of pyridoxine (CELMUC),[142] which is indicative of another dimension to the variable hydrogen-bonded chemistry of pyridoxine. Upon proton transfer all previous motifs are broken with the only exception being the retention of the intramolecular hydrogen bond between the phenolic substituent and the *para*-hydroxy group (Figure 74).
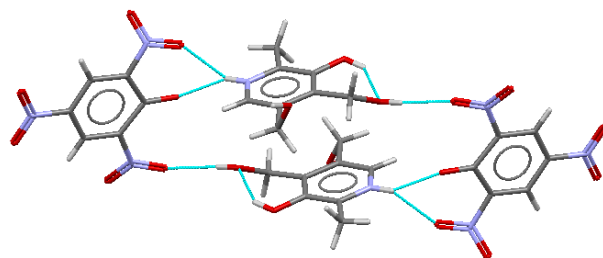
Figure 74. The structure of pyridoxinium picrate (CELMUC).[142]

Biotin reveals the presence of a stable $R_2^2(8)$ acid-amide dimer as the hydrogen-bonded interaction for both carboxylic acids groups (BIOTIN01). Their presence, at opposite ends of the molecule, give rise to head-to-tail interactions and the formation of infinite 1-D chains (Figure 75).[143] These chains are linked to each other *via* multiple imidazole N-H···O=C acid hydrogen bonds.
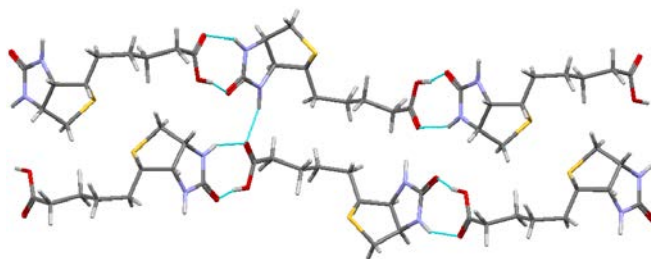
Figure 75. The structure of biotin (BIOTIN01).[143]

An examination of the structures of *D*-isoascorbic acid (IASCOR10) (Figure 76)

[144] and *L*-ascorbic acid (LASCAC12) (Figure 77)[145] reveals that identical hydrogen bonds between the hydroxy group and the enediol moiety (alcohol O-H···O alcohol and alcohol O-H···O=C enediol) are observed in both the compounds. Despite the similar intermolecular interactions in the solid-state, the two supramolecular architectures derived from the diastereomeric compounds are different from each other.
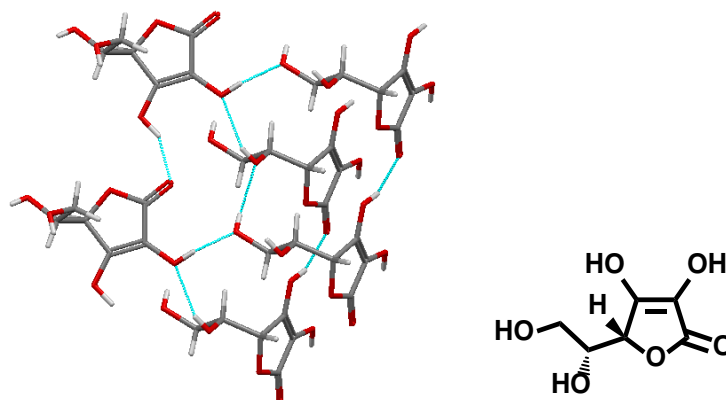
Figure 76. The structure of *D*-isoascorbic acid (IASCOR10).[144]
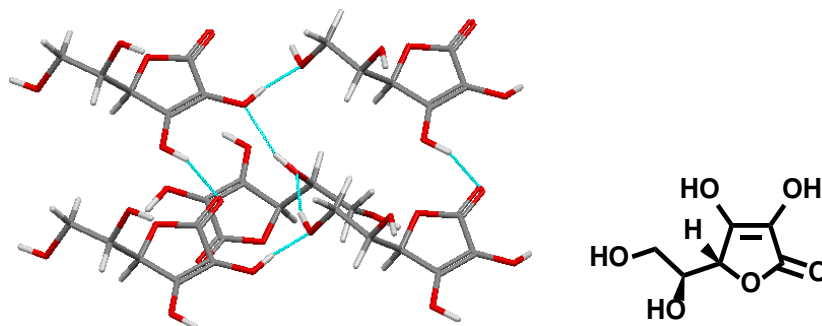
Figure 77. The structure of *L*-ascorbic acid (LASCAC12).[145]

Cholecalciferol (vitamin D_3) is a chemically and physically unstable vitamin due to the presence of the unstable conjugated triene group that is capable of undergoing topochemical reactions.[146] The structure of cholecalciferol displays hydrogen-bonded alcohol O-H···O alcohol C(2) catemeric chains (CHOCAL) (Figure 78).[147]
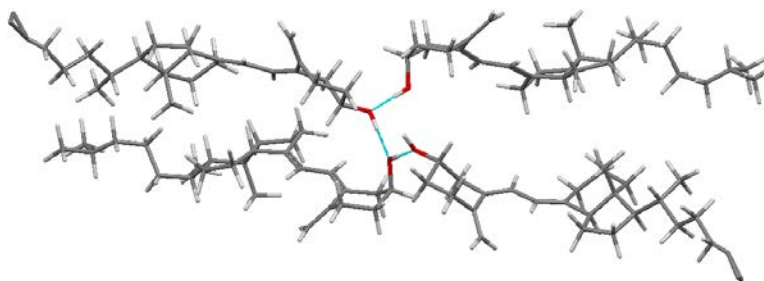
Figure 78. The structure of cholecalciferol (CHOCAL).[147]

A change is observed in the supramolecular synthons upon the cocrystallization of cholecalciferol with coformers containing alcohol functional groups such as cholesterol (RINTIT) and cholestanol (RINTOZ).[146] The stable hydrogen bonded alcohol $R_4^4(8)$ tetramers are observed for both the 1:1 cocrystals, wherein the O-H moieties of both cholecalciferol and the coformers arrange in a head-to-tail fashion, thus replacing the hydrogen-bonded chains in cholecalciferol alone (Figure 79).[146]
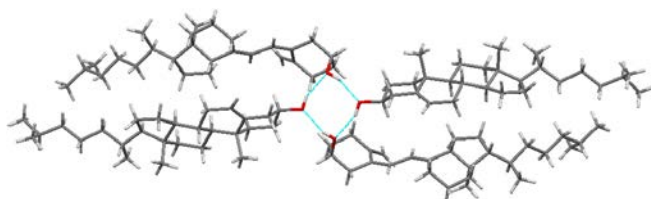
Figure 79. The structure of 1:1 cholecalciferol-cholesterol cocrystal (RINTIT).[146]

Ergocalciferol (vitamin D_2) is very similar in molecular structure to cholecalciferol. Consequently, the structure of ergocalciferol shows the similiar structural features to that of cholecalciferol with infinite 1-D chains propagated by alcohol O-H···O alcohol hydrogen bonds (ERGCAL10) (Figure 80). [148]
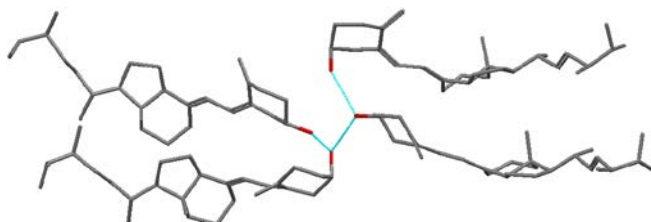
Figure 80. The structure of ergocalciferol (ERGCAL10). [148]

A 1:1 lumisterol$_2$: 6-s-trans-vitamin D_2 (ergocalciferol) composition is also known as vitamin D_1, and the structure of this cocrystal retains similar alcohol C(2) catemeric chains to those observed in ergocalciferol alone (SEQNIL) (Figure 81). [149]
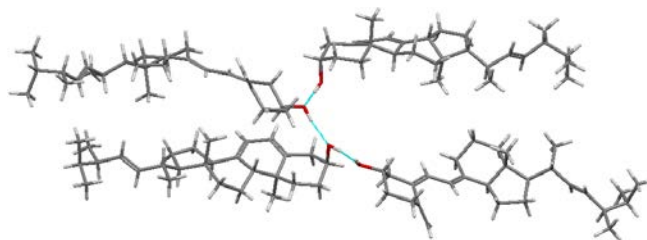
Figure 81. The structure of vitamin D_1 (SEQNIL).[149]

Folic acid dihydrate displays two key intermolecular interactions: (a) acid-amide $R_2^2(8)$ heterodimer; and (b) acid-2-aminopyridine $R_2^2(8)$ heterodimer (Figure 82).[150] The water molecules are satisfying the remaining hydrogen bond donors and acceptors.
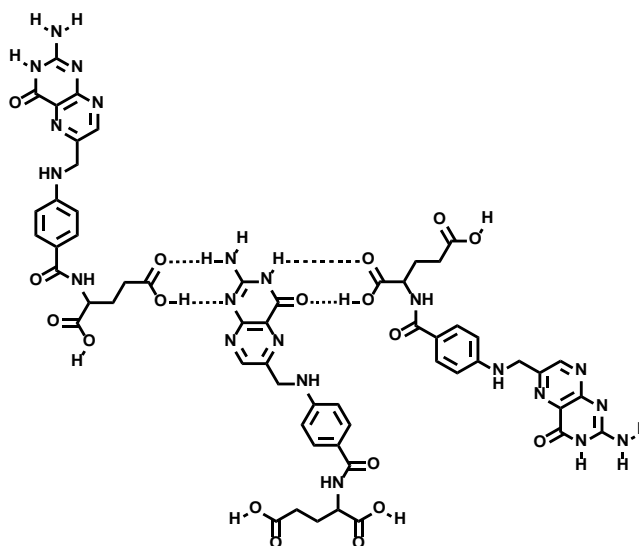
Figure 82. Hydrogen bonding motifs present in the folic acid dihydrate.[150]

The two polymorphs of menadione (IVEJUO and IVEJUO03) display no discernible hydrogen bonds in the crystalline lattice, and the supramolecular architecture is assembled *via* weak C-H$^{..}$O=C contacts along with π-π stacking present (Figure 83).[151,152]
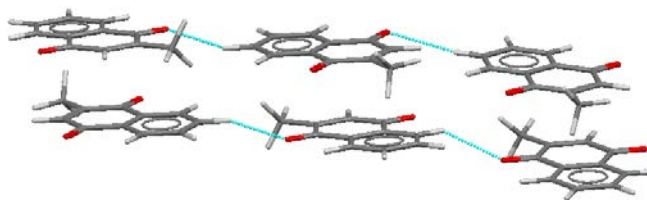
Figure 83. The structure of menadione (IVEJUO).[151]

The diverse chemical functionalities seen in the vitamins, allied with the few examples of vitamin containing cocrystals, means that a systematic analysis of their solid state behavior is presently not possible.

4. Tuning physicochemical properties

Although the cocrystallization of nutraceuticals from a pharmaceutical perspective is a relatively new field, there have been some important studies that have explored the possibility of improving key physicochemical properties such as physical stability,[51,64,87,88,92,97,146] solubility[61,62,87,88,96,112] and bioavailability[96,112] of nutraceuticals, as well as of APIs. A summary of these studies is provided in Tables 4-5 and case studies discussed in more detail below.

Table 4. Altered physicochemical properties of cocrystals of phenolic acids.[a]

Molecule	Coformer	Observations
Gallic acid	(S)-Oxiracetam[51]	Improved physical stability over both time and relative humidity.
	(±)-Oxiracetam[51]	Improved physical stability over both time and relative humidity.
	Isoniazid[52]	Difference in proton conduction upon dehydration (x 10^3).
	Pyrazine-2-carboxamide.H_2O[61]	Increased aqueous solubility (x 1.3).
Protocatechuic acid	(S)-Oxiracetam[51]	Altered physical stability over both time and relative humidity.
	(±)-Oxiracetam[51]	Altered physical stability over both time and relative humidity.
Vanillic acid	Pyrazine-2-carboxamide[61]	Increased aqueous solubility (x 2.2).
	Ethenzamide[62]	Improved equilibrium solubility (x 4.5) and intrinsic dissolution rate (x 1.7).
	Andrographolide[64]	Improved chemical stability of andrographolide.

[a] relative to the nutraceutical

Table 5. Altered physicochemical properties of stilbene and flavonoid cocrystals.[a]

Molecule	Coformer	Observations
Pterostilbene	Piperazine[87]	Improved physical stability over both time and relative humidity; increased aqueous solubility (x 6).
	Glutaric acid[87]	Improved physical stability over both time and relative humidity.
	Caffeine (Form I) [88]	Improved physical stability over both time and relative humidity; increased solubility (x 27).
	Carbamazepine[88]	Improved physical stability over both time and relative humidity; decreased solubility (x 2.5).

Myricetin	Piracetam[92]	Reduced thermal stability.
Quercetin	Isonicotinamide[96]	Increased solubility (x 5); increased bioavailability (x 6), reaches systemic circulation faster.
	Theobromine.$2H_2O$[66,96]	Improved solubility; increased bioavailability (x 10), slower elimination from the body.
	Caffeine[96]	Increased solubility (x 14); increased bioavailability (x 3).
	Caffeine.CH_3OH[96]	Increased solubility (x 8); increased bioavailability (x 4).
Fisetin	Isonicotinamide[97]	Reduced thermal stability.
	2Nicotinamide.$0.5C_2H_5OH$[97]	Reduced thermal stability.
	Nicotinamide[97]	Reduced thermal stability.
Luteolin	Isonicotinamide (Forms I and II) [97]	Reduced thermal stability.
Genistein	Nicotinamide.H_2O[97]	Reduced thermal stability.
Epicatechin gallate (ECG)	2Caffeine.$3H_2O$[110]**Error! Bookmark not defined.**	Improved aqueous stability.
Epigallocatechin gallate (EGCG)	Nicotinamide.$9H_2O$[112]	Decreased solubility (x 8); decreased bioavailability (45%).
	Isonicotinamide.$5H_2O$[112]	Decreased solubility (x 17); decreased bioavailability (40%).
	Isonicotinic acid.$3H_2O$[112]	Decreased solubility (x 22); increased bioavailability ($F_{rel} = 1.37$).
	Isonicotinic acid[112]	Decreased solubility (x 19); increased bioavailability ($F_{rel} = 1.05$).

[a] relative to the nutraceutical

Physicochemical properties such as solubility and dissolution rate were evaluated for cocrystals of vanillic acid (**3**) with the analgesic drug ethenzamide in 10% ethanol-water (v/v). [62] There is a 4.5 fold improvement in the equilibrium solubility of 1:1 ethenzamide:vanillic acid cocrystal (7.12 mg mL^{-1}) in comparison to ethenzamide (1.58 mg mL^{-1}). Also, the intrinsic dissolution rate (IDR) of the cocrystal is 1.7 times (7.55 x 10^{-3} mg cm^{-2} min^{-1}) that of ethenzamide alone (4.40 x 10^{-3} mg cm^{-2} min^{-1}). Cocrystals containing gallic acid (**1**) and the API (*S*)-oxiracetam / (*RS*)-oxiracetam show much improved hygroscopic stability over prolonged periods of time relative to the API.[51] The (*S*) enantiomer is stable up to 75% relative humidity (RH) for eight weeks, whereas racemic oxiracetam is stable up to 87% RH for eight weeks. In comparison, gallic acid cocrystals with either enantiopure or racemic oxiracetam are stable up to 98% RH for eight weeks. This significant enhancement in the hygroscopic stability has been attributed to the formation of a more extended 3D hydrogen bonded framework in these cocrystals.

Pterostilbene (**10**), a nutraceutical having poor aqueous solubility (21 µg mL^{-1}) was cocrystallized with four pharmaceutically acceptable coformers, *viz* caffeine, carbamazepine, glutaric acid and piperazine, to improve its aqueous solubility.[87,88] Although the cocrystals with caffeine, carbamazepine and piperazine resulted in lower solubility of the coformers, the concentration of pterostilbene achieved in solution was increased 27-fold for the cocrystal with caffeine, whereas it was lowered 2.5-fold for the cocrystal with carbamazepine. All the cocrystals in this study displayed remarkable physical stability, with respect to increasing RH and temperature over specified time periods of up to 8 weeks, in comparison to the individual coformers.

Quercetin (**12**), one of the most abundant flavonoids in the plant kingdom, is well known for its numerous therapeutic bioactivities *in vitro*. However, its efficacy is limited *in vivo* due to the poor bioavailability and low solubility. The physicochemical properties (solubility and bioavailability) of four cocrystals of quercetin with GRAS coformers (isonicotinamide, theobromine and caffeine) were examined in 50% ethanol-water (v/v), and it was found that each of these cocrystals exhibited superior solubility compared to quercetin dihydrate (Table 4). [96] It was hypothesized that an improvement in solubility would translate into enhanced systemic absorption of quercetin, and the experimental results validated this hypothesis as up to a 10-fold improvement in the bioavailability was observed in comparison to quercetin dihydrate (see F_{rel} values in Table 6). This study suggests that cocrystallization can be a potential solution to the solubility and bioavailability problems that prevent **12** from being used as an effective treatment option for its numerous therapeutic bioactivities.

Table 6. Solubility and bioavailability (F_{rel}) of **12** and its cocrystals.[96]

	12	**12**:Isonicotinamide	**12**:Caffeine.MeOH	**12**:Caffeine	**12**:Theobromine.2H_2O
Solubility (mg mL^{-1})	0.267	1.22	2.018	3.627	0.326
F_{rel}	1.00	5.46	4.01	2.57	9.93

Five cocrystals of the flavonoids fisetin (**13**), luteolin (**14**) and genistein (**18**), natural polyphenolic compounds of pharmaceutical interest, were synthesized with nicotinamide and isonicotinamide as coformers.[97] An examination of the thermal stability of **13**:isonicotinamide and **14**:isonicotinamide (Forms I and II) revealed that the cocrystals were stable up to 230, 250 and 260 ºC, respectively. The solvated **13**:nicotinamide and **18**:nicotinamide exhibit loss of

solvent molecules above 110 and 80 ℃, respectively, with the desolvated **13**:nicotinamide cocrystal being further stable up to 180 ℃. The melting point of these cocrystals lies in between that of the flavonoid and the coformer, and the authors refer to this as a reduction in thermal stability with respect to the flavonoid.

Cholecalciferol/vitamin D_3 (**31**) is a chemically and physically unstable vitamin used for the treatment of osteomalacia and osteoporosis.[153] The unstable conjugated triene group undergoes topochemical reactions, as a result it has to be stored under controlled conditions and is rarely formulated in solid dosage form. Two cocrystals of **31** with pharmaceutically acceptable steroids, cholesterol and cholestanol, have been prepared utilizing O-H$^{...}$O hydrogen bonds.[146] These isostructural cocrystals are topochemically stable and have a far superior chemical and physical stability compared to **31** alone. An increased packing coefficient (C_k = 0.702 and 0.696 for **31**:cholesterol and **31**:cholestanol, respectively) and density (1.06 and 1.05 g/cm^3 for **31**:cholesterol and **31**:cholestanol, respectively) is responsible for imparting increased conformational stability to the cocrystals. Also, the two cocrystals show improved thermal stability (by 40 ℃), and physical stability over both time and RH. These results may encourage the future development of novel forms of this important bioactive vitamin and facilitate its widespread use in nutrition industries.

5. Summary and Outlook

Pharmaceutical cocrystallization is an important and rapidly expanding field with the objective of favorably altering the physical properties of APIs. The choice of the coformer is crucial in cocrystallization not only for synthon compatibility, but also because properties of the obtained multi-component materials are generally strongly influenced by the coformer. Usually the

accepted coformers are chosen from the GRAS or EAFUS lists. Nutraceuticals are a class of compounds that are readily available over the counter, are easily patentable, and have a wide range of beneficial properties (*e.g.* anti-oxidants), however, they are yet to be utilized extensively as coformers in cocrystallization. In this review, we have detailed the different forms of nutraceuticals that have been explored to date and analyzed the different inter- and intramolecular interactions involved in their solid state forms.

There are two categories of nutraceuticals, namely polyphenols and vitamins, of which polyphenols can be further subdivided into (i) phenolic acids and (ii), coumarin, stilbenes, flavonoids and lignans. All the observed crystal structures have been divided into six categories (pure compounds, hydrated structures, cocrystals, hydrated cocrystals, salts, and solvates) to help better understand the available data and to aid in the analysis of the different motifs present in their solid state structures. Upon examination of the data it is observed that, relatively, phenolic acids have been studied in greater detail, followed by flavonoids, and the least explored are the vitamins. Notably, the key supramolecular motifs observed in the structures of nutraceuticals, either pure or in cocrystals, are entirely as expected based on established supramolecular synthons. For phenolic acids, which combine carboxylic acid and phenolic substituents, the acid-acid dimer is generally seen, particularly in the absence of any competing hydrogen bond donors or acceptors. The phenolic substituents form O-H$\cdots$O homosynthons or are hydrogen bonded to the acid-acid dimer. The presence of competing hydrogen bond donors and acceptors often disrupts the acid-acid dimer motif with hydrogen bonding occurring according to Etter's rules. Flavonoids only have phenolic substituents on the backbone, and hence primarily form phenol O-H$\cdots$O phenol homosynthons in the solid state. Addition of coformers allows a variety of supramolecular motifs such as phenol O-H$\cdots$N$_{arom}$, and phenol O-H$\cdots$O=C acid/amide/ketone

hydrogen bonds to be exploited for cocrystallization. Vitamins have a diverse range of functional groups and, accordingly, their supramolecular chemistry is a direct reflection of the groups present.

A handful of studies have explored the cocrystallization of APIs with nutraceuticals with a view to favorably altering the physicochemical properties of APIs, such as physical stability, solubility, and bioavailability. Greater emphasis has been given to the thermal stability and the physical stability of these cocrystals over a wide range of time and humidity, with remarkable success being achieved in the case of gallic acid, protocatechuic acid, pterostilbene, myricetin, luteolin, genistein, and fisetin. The solubility and bioavailability have also been successfully altered for some nutraceuticals including phenolic acids, stilbenes and flavonoids.

The field of cocrystallization of nutraceuticals is still in its infancy. Knowledge of the different solid state forms of nutraceuticals and the supramolecular synthons commonly observed in their structures, which have been described in this review, will allow the formation of functional materials with targeted physicochemical properties in the future, for example, exploiting the anti-oxidant properties of flavonoids and other nutraceuticals. Furthermore, ionic cocrystals in which a salt is cocrystallized with either an organic molecule, or an organic salt, have received considerable attention recently,[154-157] and nutraceuticals are an obvious candidate for this area of study. In summary, this review assesses the structural data available to date across a diverse range of nutraceuticals, both in pure form and in multicomponent materials, and identifies the persistent supramolecular features present. It provides a firm foundation for future studies which will ultimately enable predictive and controlled assembly of functional materials incorporating nutraceuticals together with APIs.

Supporting Information Available Calculated molecular electrostatic potentials. This information is available free of charge via the Internet at http://pubs.acs.org/.

*Corresponding author: Simon E. Lawrence

Address: Department of Chemistry, Analytical and Biological Chemistry Research Facility, Synthesis and Solid State Pharmaceutical Centre, University College Cork, Cork, Ireland

Email: s.lawrence@ucc.ie. Tel.: +353 21 490 3143

References

1   Aakeröy, C. B.; Salmon, D. J. *CrystEngComm* **2005**, *7*, 439.

2   Aitipamula, S.; Banerjee, R.; Bansal, A. K.; Biradha, K.; Cheney, M. L.; Choudhury, A. R.; Desiraju, G. R.; Dikundwar, A. G.; Dubey, R.; Duggirala, N.; Ghogale, P. P.; Ghosh, S.; Goswami, P. K.; Goud, N. R.; Jetti, R. R. K. R.; Karpinski, P.; Kaushik, P.; Kumar, D.; Kumar, V.; Moulton, B.; Mukherjee, A.; Mukherjee, G.; Myerson, A. S.; Puri, V.; Ramanan, A.; Rajamannar, T.; Reddy, C. M.; Rodriguez-Hornedo, N.; Rogers, R. D.; Row, T. N. G.; Sanphui, P.; Shan, N.; Shete, G.; Singh, A.; Sun, C. C.; Swift, J. A.; Thaimattam, R.; Thakur, T. S.; Thaper, R. K.; Thomas, S. P.; Tothadi, S.; Vangala, V. R.; Variankaval, N.; Vishweshwar, P.; Weyna, D. R.; Zaworotko, M. J. *Cryst. Growth Des.* **2012**, *12*, 2147–2152.

3   Blagden, N.; Coles, S. J.; Berry, D. J. *CrystEngComm* **2014**, *16*, 5753-5761.

4   Steed, J. W. *Trends Pharmacol. Sci.* **2013**, *34*, 185-193.

5   Brittain, H. G. *J. Pharm. Sci.* **2013**, *102*, 311-317.

6   Brittain, H. G. *Cryst. Growth Des.* **2012**, *12*, 5823-5832.

7   Schultheiss, N.; Newman, A. *Cryst. Growth Des.* **2009**, *9*, 2950-   2967.

8   Shan, N.; Zaworotko, M. J. *Drug Discov. Today* **2008**, *13*, 440-446.

9   Crystal   Growth   and   Design   'virtual   issue'   on   cocrystals: http://pubs.acs.org/page/cgdefu/vi/1.

10   Sanphui, P.; Tothadi, S.; Ganguly, S.; Desiraju, G. R. *Mol. Pharmaceutics* **2013**, *10*, 4687–4697.

11   Good, D. J.; Rodríguez-Hornedo, N. *Cryst. Growth Des.* **2009**, *5*, 2252-2264.

12   Aakeröy, C. B.; Forbes, S.; Desper, J. *J. Am. Chem. Soc.* **2009**, *131*, 17048-17049.

13   Shiraki, K.; Takata, N.; Takano, R.; Hayashi, Y.; Terada, K. *Pharmacol. Res.* **2008**, *25*, 2581-2592.

14   Trask, A. V.; Samuel Motherwell, W. D.; Jones, W. *Int. J. Pharm.* **2006**, *320*, 114-123.

15   Rodríguez-Hornedo, N.; Nehm, S. J.; Jayasankar, A. Cocrystals: Design, Properties, and Formation Mechanisms, in *Encyclopedia of Pharmaceutical Technology*, ed. Swarbrick, J., Informa Healthcare USA, 3rd edn., 2006.

16   Trask, A. V.; Samuel Motherwell, W. D.; Jones, W. *Cryst. Growth Des.* **2005**, *5*, 1013-1021

17 Cheney, M. L.; Shan, N.; Healy, E. R.; Hanna, M.; Wojtas, L.; Zaworotko, M. J.; Sava, V.; Song, S.; Sanchez-Ramos, J. R. *Cryst. Growth Des.* **2010**, *10*, 394-405.

18 Hickey, M. B.; Peterson, M. L.; Scoppettuolo, L. A.; Morrisette, S. L.; Vetter, A.; Guzmán, H.; Remenar, J. F.; Zhang, Z.; Tawa, M. D.; Haley, S.; Zaworotko, M. J.; Almarsson, Ö. *Eur. J. Pharm. Biopharm.* **2007**, *67*, 112-119.

19 McNamara, D. P.; Childs, S. L.; Giordano, J.; Iarriccio, A.; Cassidy, J.; Shet, M. S.; Mannion, R.; Park, A. *Pharmacol. Res.* **2006**, *23*, 1888-1898.

20 Nauha, E. Crystalline forms of selected agrochemical actives: design and synthesis of co-crystals. Department of Chemistry, University of Jyväskylä / Research report No. 151, 2012.

21 http://www.fda.gov/downloads/Drugs/GuidanceComplianceRegulatoryInformation/ Guidances/ucm281764.pdf.

22 Generally Regarded as Safe: http://www.cfsan.fda.gov/~rdb/opagras.html and http://www.cfsan.fda.gov/~dms.grasguid.html.

23 *Handbook of Pharmaceutical Salts: Properties, Selection and Use*, ed. Stahl, P. H.; Wermuth, C. G., Verlag Helvetica Chimica Acta, Zürich, 2002.

24 Brower V. *Nat Biotechnol.* **1998**, *16*, 728-731.

25 Zeisel S. H. *Science* **1999**, *285*, 1853-1855.

26 Kalra, E. K. *AAPS PharmSci.* **2003**, *5*, e25.

27 Munin, A.; Edwards-Lévy, F. *Pharmaceutics* **2011**, *3*, 793-829.

28   http://www.health.harvard.edu/newsweek/Listing_of_vitamins.htm.

29   Massaro, M.; Scoditti, E.; Carluccio, M. A.; De Caterina, R. *Cardiovasc. Ther.* **2010**, *28*, e13-9.

30   Pandey, M.; Verma, R. K.; Saraf, S. A. *Asian J. Pharm. Clin. Res.* **2010**, *3*, 11-15.

31   Sekhon, B. S. *RGUHS J. Pharm. Sci.* **2012**, *2*, 16-25.

32   Sun, C. C. *Expert Opin. Drug Deliv.* **2013**, *10*, 201-213.

33   Thakuria, R.; Delori, A.; Jones, W.; Lipert, M. P.; Roy, L.; Rodríguez-Hornedo, N. *Int. J. Pharm.* **2013**, *453*, 101-125.

34   Sanphui, P.; Goud, N. R.; Khandavilli, U. B. R.; Nangia, A. *Cryst. Growth Des.* **2011**, *11*, 4135-4145.

35   Babu, N. J.; Nangia, A. *Cryst. Growth Des.* **2011**, *11*, 2662-2679.

36   Lewandowska, U.; Szewczyk, K.; Hrabec, E.; Janecka, A.; Gorlach, S. *J. Agric. Food Chem.* **2013**, *61*, 12183-12199.

37   Najar, A. A.; Azim, Y. *J. Indian I. Sci.* **2014**, *94*, 45-67.

38   Friščić, T; Jones, W. *J. Pharm. Pharmacol.* **2010**, *62*, 1547-1559.

39   Allen, F. H. *Acta. Crystallogr. B* **2002**, *B58*, 380-388.

40   CSD ConQuest 1.16. (May 2014).

41   Garavello, W.; Rossi1, M.; McLaughlin, J. K.; Bosettil, C.; Negri1, E.; Lagiou, P.; Talamini, R.; Franceschi, S.; Parpinel, M.; Dal Maso, L.; La Vecchia1, C. *Annals of Oncology* **2007**, *18*, 1104–1109.

42   Rice-Evans, C. A.; Miller, N. J.; Paganga, G. *Biol. Med.* **1996**, *20*, 933-956.

43   Korkina, L.; G.; Afanasev, I. B. *Adv. Pharmacol*. **1997**, *38*, 151-163.

44   Etter, M. C. *Acc. Chem. Res.* **1990**, *23*, 120-126.

45   Bernstein, J.; Davis, R. E.; Shimoni, L.; Chang, N.-L. *Angew. Chem., Int. Ed. Engl.* **1995**, *34*, 1555-1573.

46   Braun, D. E.; Bhardwaj, R. M.; Florence, A. J.; Tocher, D. A.; Price, S. L. *Cryst. Growth Des.* **2013**, *13*, 19-23.

47   Clarke, H. D.; Arora, K. K.; Wojtas, L.; Zaworotko, M. J. *Cryst. Growth Des.* **2011**, *11*, 964-966.

48   Okabe, N.; Kyoyama, H.; Suzuki, M. *Acta Crystallogr. E* **2001**, *E57*, 764-766.

49   Jiang, R.-W.; Ming, D.-S.; But, P. P. H.; Mak, T. C. W. *Acta Crystallogr. C* **2000**, *C56*, 594-595.

50   Kaur, R.; Row, T. N. G. *Cryst. Growth Des.* **2012**, *12*, 2744-2747.

51   Wang, Z.-Z.; Chen, J.-M.; Lu, T.-B. *Cryst. Growth Des.* **2012**, *12*, 4562-4566.

52   Kaur, R.; Perumal, S. S. R. R.; Bhattacharyya, A. J.; Yashonath, S.; Row, T. N. G. *Cryst. Growth Des.* **2014**, *14*, 423-426.

53   Etter, M. C. *J. Phys. Chem.* **1991**, *95*, 4601-4610.

54   Etter, M. C.; Frankenbach, G. M. *Chem. Mater.* **1989**, *1*, 10-12.

55   Donohue, J. *J. Phys. Chem.* **1952**, *56*, 502-510.

56   Sarma, B.; Sanphui, P.; Nangia, A. *Cryst. Growth Des.* **2010**, *10*, 2388-2399.

57   Desiraju, G. R. *Angew. Chem., Int. Ed. Engl.* **1995**, *34*, 2311-2327.

58   Horneffer, V.; Dreisewerd, K.; Ludemann, H.-C.; Hillenkamp, F.; Lage, M.; Strupat, K. *Int. J. Mass Spectrom.* **1999**, *185*, 859-870.

59   Ng, S. W. *Acta Crystallogr. E* **2011**, *E67*, o2476.

60   Kozlevčar, B.; Odlazek, D.; Golobič, A.; Pevec, A.; Strauch, P.; Šegedin, P. *Polyhedron* **2006**, *25*, 1161-1166.

61   Adalder, T. K.; Sankolli, R.; Dastidar, P. *Cryst. Growth Des.* **2012**, *12*, 2533-2542.

62   Aitipamula, S.; Wong, A. B. H.; Chow, P. S.; Tan, R. B. H. *CrystEngComm* **2012**, *14*, 8515-8524.

63   Aakeröy, C. B.; Hurley, E. P.; Desper, J. *Cryst. Growth Des.* **2012**, *12*, 5806-5814.

64   Suresh, K.; Goud, N. R.; Nangia, A. *Chem. Asian J.* **2013**, *8*, 3032-3041.

65   Lombardo, G. M.; Portalone, G.; Colapietro, M.; Rescifina, A.; Punzo, F. *J. Mol. Struct.* **2011**, *994*, 87-96.

66   Clarke, H. D.; Arora, K. K.; Bass, H.; Kavuru, P.; Ong, T. T.; Pujari, T.; Wojtas, L.; Zaworotko, M. J. *Cryst. Growth Des.* **2010**, *10*, 2152-2167.

67   Bryan, R. F.; Forcier, P. G. *Mol. Cryst. Liq. Cryst.* **1980**, *60*, 157-165.

68   Schultheiss, N.; Roe, M.; Boerrigter, S. X. M. *CrystEngComm* **2011**, *13*, 611-619.

69   Ravikumar, N.; Gaddamanugu, G.; Solomon, K. A. *J. Mol. Struct.* **2013**, *1033*, 272-279.

70   Bevill, M. J.; Vlahova, P. I.; Smit, J. P. *Cryst. Growth Des.* **2014**, *14*, 1438-1448.

71   Thomas, S. P.; Pavan, M. S.; Row T. N. G. *Cryst. Growth Des.* **2012**, *12*, 6083-6091.

72   Tan, Z.; Zhu, E.; Luo, L.; Lin, Z.; Yan, R. *Acta Crystallogr. E* **2011**, *67*, o424.

73   Aakeröy, C. B.; Beatty, A. M.; Helfrich, B. A. *Angew. Chem., Int. Ed.* **2001**, *40*, 3240-3242.

74   Shattock, T. R.; Arora, K. K.; Vishweshwar, P.; Zaworotko, M. J. *Cryst. Growth Des.* **2008**, *8*, 4533-4545.

75   Laurence, C.; Berthelot, M.; Graton, J. Hydrogen-Bonded Complexes of Phenols. In *Phenols*; Rappoport, Z., Ed.; John Wiley & Sons, Ltd.: Chichester, U.K., **2003**.

76   Ermer, O.; Eling, A. *J. Chem. Soc., Perkin Trans. 2* **1994**, 925-944.

77   Bordwell, F. G.; McCallum, R. J.; Olmstead, W. N. *J. Org. Chem.* **1984**, 49, 1424-1427.

78   Hadzi, D.; Detoni, S. Hydrogen bonding in carboxylic acids and derivatives. In *Acid Derivatives*, Vol. 1; Patai, S., Ed.; John Wiley & Sons, Ltd.: Chichester, U.K., **1979**.

79   Hamilton, W. C.; Ibers, J. A. *Hydrogen Bonding in Solids*; W. A. Benjamin: New York, **1968**.

80   Aakeröy, C. B.; Epa, K.; Forbes, S.; Schultheiss, N.; Desper, J. *Chem. Eur. J.* **2013**, *19*, 14998-15003.

81   Hou, G.-G.; Ma, J.-P.; Wang, L.; Wang, P.; Dong, Y.-B.; Huang, R.-Q. *CrystEngComm* **2010**, *12*, 4287-4303.

82   Harborne, J. B.; Williams, C. A. *Phytochemistry* **2000**, *55*, 481-504.

83   Erlund, I. *Nutr. Res.* **2004**, *24*, 851-874.

84   Kimura, M.; Watson, W. H. *Cryst. Struct. Commun.* **1980**, *9*, 257.

85   Beh, H.-K.; Ismail, Z.; Asmawi, M. Z.; Loh, W.-S.; Fun, H.-K. *Acta Crystallogr. E* **2010**, *66*, o2138.

86   Caruso, F.; Tanski, J.; Villegas-Estrada, A.; Rossi, M. *J. Agric. Food Chem.* **2004**, *52*, 7279-7285.

87   Bethune, S. J.; Schultheiss, N.; Henck, J.-O. *Cryst. Growth Des.* **2011**, *11*, 2817-2823.

88   Schultheiss, N.; Bethune, S.; Henck, J.-O. *CrystEngComm* **2010**, *12*, 2436-2442.

89   http://www.iupac.org/home/publications/provisional-recommendations/under-review-by-the-authors/under-review-by-the-authors-container/nomenclature-of-flavonoids.html.

90   Beecher, G. R. *J. Nutr.* **2003**, *133*, 3248S-3254S.

91   Cody, V.; Luft, J. R. *J. Mol. Struct.* **1994**, *317*, 89-97.

92   Sowa, M.; Ślepokura, K.; Matczak-Jon, E. *J. Mol. Struct.* **2014**, *1058*, 114-121.

93   Domagala, S.; Munshi, P.; Ahmed, M.; Guillot, B.; Jelsch, C. *Acta Crystallogr. B* **2011**, *B67*, 63-78.

94   Jin, G.-Z.; Yamagata, Y.; Tomita, K. *Acta Crystallogr. C* **1990**, *C46*, 310-313.

95   Timmons, D. J.; Pacheco, M. R.; Fricke, K. A.; Slebodnick, C. *Cryst. Growth Des.* **2008**, *8*, 2765-2769.

96   Smith, A. J.; Kavuru, P.; Wojtas, L.; Zaworotko, M. J.; Shytle, R. D. *Mol. Pharmaceutics* **2011**, *8*, 1867-1876.

97   Sowa, M.; Ślepokura, K.; Matczak-Jon, E. *CrystEngComm* **2013**, *15*, 7696-7708.

98   Cox, P. J.; Kumarasamy, Y.; Nahar, L.; Sarker, S. D.; Shoeb, M. *Acta Crystallogr. E* **2003**, *59*, o975.

99   Aitipamula, S.; Chow, P. S.; Tan, R. B. H. *CrystEngComm* **2009**, *11*, 1823-1827.

100   Goswami, P. K.; Thaimattam, R.; Ramanan, A. *Cryst. Growth Des.* **2013**, *13*, 360-366.

101   Hibbs, D. E.; Overgaard, J.; Gatti, C.; Hambley, T. W. *New J. Chem.* **2003**, *27*, 1392-1398.

102   Sowa, M.; Ślepokura, K.; Matczak-Jon, E. *Acta Crystallogr. C* **2012**, *C68*, o262-o265.

103   Shin, W.; Lah, M. S. *Acta Crystallogr. C* **1986**, *42*, 626-628.

104   Fujii, S.; Yamagata, Y.; Jin, G.-Z.; Tomita, K. *Chem. Pharm. Bull.* **1994**, *42*, 1143.

105   Shin, W.; Kim, S.; Chun, K. S. *Acta Crystallogr. C* **1987**, *43*, 1946-1949.

106   Breton, M.; Precigoux, G.; Courseille, C.; Hospital, M. *Acta Crystallogr. B* **1975**, *31*, 921-923.

107   Sowa, M.; Ślepokura, K.; Matczak-Jon, E. *Acta Crystallogr. C* **2013**, *69*, 1267-1272.

108   Fronczek, F. R.; Gannuch, G.; Mattice, W. L.; Tobiason, F. L.; Broeker, J. L.; Hemingway, R. W. *J. Chem. Soc., Perkin Trans. 2* **1984**, 1611-1616.

109   Harper, J. K.; Doebbler, J. A.; Jacques, E.; Grant, D. M.; Von Dreele, R. B. *J. Am. Chem. Soc.* **2010**, *132*, 2928-2937.

110   Ishizu, T.; Sato, T.; Tsutsumi, H.; Yamamoto, H. *Chem. Lett.* **2010**, *39*, 607-609.

111   Tsutsumi, H.; Kinoshita, Y.; Sato, T.; Ishizu, T. *Chem. Pharm. Bull.* **2011**, *59*, 1008-1015.

112   Smith, A. J.; Kavuru, P.; Arora, K. K.; Kesani, S.; Tan, J.; Zaworotko, M. J.; Shytle, R. D. *Mol. Pharmaceutics* **2013**, *10*, 2948-2961.

113   Ishizu, T.; Tsutsumi, H.; Sato, T.; Yamamoto, H.; Shiro, M. *Chem. Lett.* **2009**, *38*, 230-231.

114   Ishizu, T.; Tsutsumi, H.; Sato, T. *Tetrahedron Lett.* **2009**, *50*, 4121-4124.

115   Tsutsumi, H.; Sato, T.; Ishizu, T. *Chem. Lett.* **2012**, *41*, 1669-1671.

116   Lundquist, K.; Stomberg, R. *Holzforschung* **1988**, *42*, 375.

117   Stomberg, R.; Langer, V.; Li, S.; Lundquist, K. *Acta Crystallogr. E* **2001**, *57*, o692-o694.

118   Kraus, G. A.; Wu, Y. *J. Org. Chem.* **1992**, *57*, 2922-2925.

119 Chandramohan, K.; Ravikumar, K.; Damayanthi, Y.; Kamal, A. *Z. Kristallogr.* **2000**, *215*, 45.

120 Eddleston, M. D.; Madusanka, N.; Jones, W. *J. Pharm. Sci.* **2014**. doi: 10.1002/jps.24003.

121 Trask, A. V.; Motherwell, W. D. S.; Jones, W. *Cryst. Growth Des.* **2005**, *5*, 1013-1021.

122 Reutzel-Edens, S. M.; Bush, J. K.; Magee, P. A.; Stephenson, G. A.; Byrn, S. R. *Cryst. Growth Des.* **2003**, *3*, 897-907.

123 Desiraju, G. R. *J. Chem. Soc., Chem. Commun.* **1991**, 426-428.

124 Infantes, L.; Chisholm, J.; Motherwell, S. *CrystEngComm* **2003**, *5*, 480-486.

125 van de Streek, J.; Motherwell, S. *CrystEngComm* **2007**, *9*, 55-64.

126 Lieberman, S.; Bruning, N. The Real Vitamin & Mineral Book; Avery Publishing Group: New York, 1990.

127 Fortmann, S. P.; Burda, B. U.; Senger, C. A.; Lin, J. S.; Whitlock, E. P. *Ann. Intern. Med.* **2013**, *159*, 824-834.

128 Pan-Pan, Z.; Xiao-Bo, S.; Wen-Yuan, Q. *Curr. Drug Discovery Technol.* **2014**, *11*, 97-108.

129 Drikos, G.; Ruppel, H.; Dietrich, H.; Sperling, W. *FEBS Lett.* **1981**, *131*, 23-27.

130 Simmons, C. J.; Liu, R. S. H.; Denny, M.; Seff, K. *Acta Crystallogr. B* **1981**, *37*, 2197-2205.

131   Gilardi, R. D.; Karle, I. L.; Karle, J. *Acta Crystallogr. B* **1972**, *28*, 2605-2612.

132   Hamanaka, T.; Mitsui, T.; Ashida, T.; Kakudo, M. *Acta Crystallogr. B* **1972**, *28*, 214-222.

133   Simmons, C. J.; Asato, A. E.; Denny, M.; Liu, R. S. H. *Acta Crystallogr. C* **1986**, *42*, 1558-1563.

134   Malpezzi, L.; Fuganti, C.; Grasselli, P. *Acta Crystallogr. C* **1997**, *53*, 508-511.

135   Stam, C. H. *Acta Crystallogr. B* **1972**, *28*, 2936-2945.

136   Zanotti, G.; D'Acunto, M. R.; Malpeli, G.; Folli, C.; Berni, R. *Eur. J. Biochem.* **1995**, *234*, 563-569.

137   Fujii, S.; Kawasaki, K.; Sato, A.; Fujiwara, T.; Tomita, K.-I. *Arch. Biochem. Biophys.* **1977**, *181*, 363-370.

138   Hoogsteen, K. *Acta Cryst.* **1963**, *16*, 907-916.

139   Voet, D.; Rich, A. *Proc. Nat. Acad. Sci. USA* **1971**, *68*, 1151-1156.

140   Salunke, D. M.; Vijayan, M. *Biochim. Biophys. Acta* **1984**, *798*, 175-179.

141   Longo, J.; Franklin, K. J.; Richardson, M. F. *Acta Crystallogr. B* **1982**, *38*, 2721-2724.

142   Anitha, K.; Athimoolam, S.; Natarajan, S. *Acta Crystallogr. C* **2006**, *62*, o426-o428.

143   DeTitta, G. T.; Edmonds, J. W.; Stallings, W.; Donohue, J. *J. Am. Chem. Soc.* **1976**, *98*, 1920-1926.

144   Azarnia, N.; Berman, H. M.; Rosenstein, R. D. *Acta Crystallogr. B* **1972**, *28*, 2157-2161.

145 Milanesio, M.; Bianchi, R.; Ugliengo, P.; Roetti, C.; Viterbo, D. *J. Mol. Struct.: THEOCHEM* **1997**, *419*, 139-154.

146 Wang, J.-R.; Zhou, C.; Yu, X.; Mei, X. *Chem. Commun.* **2014**, *50*, 855-858.

147 Trinh-Toan; DeLuca, H. F.; Dahl, L. F. *J. Org. Chem.* **1976**, *41*, 3476-3478.

148 Hull, S. E.; Leban, I.; Main, P.; White, P. S.; Woolfson, M. M. *Acta Crystallogr. B* **1976**, *32*, 2374-2381.

149 Tan, E. S.; Tham, F. S.; Okamura, W. H. *Chem. Commun.* **2000**, 2345-2346.

150 Mastropaolo, D.; Camerman, A.; Camerman, N. *Science* **1980**, *210*, 334-336.

151 Nowell, H.; Attfield, J. P. *New J. Chem.* **2004**, *28*, 406-411.

152 Rane, S.; Ahmed, K.; Gawali, S. S.; Zaware, S. B.; Srinivas, D.; Gonnade, R.; Bhadbhade, M. *J. Mol. Struct.* **2008**, *892*, 74-83.

153 Labler, L. *Ullmann's Encyclopedia of Industrial Chemistry*, Wiley-VCH, Weinheim, 1996.

154 Childs, S. L.; Chyall, L. J.; Dunlap, J. T.; Smolenskaya, V. N.; Stahly, B. C.; Stahly, G. P. *J. Am. Chem. Soc.* **2004**, *126*, 13335-13342.

155 Braga, D.; Grepioni, F.; Maini, L.; Prosperi, S.; Gobetto, R.; Chierotti, M. R. *Chem. Commun.* **2010**, *46*, 7715-7717.

156 Ong, T. T.; Kavuru, P.; Nguyen, T.; Cantwell, R.; Wojtas, L.; Zaworotko, M. J. *J. Am. Chem. Soc.* **2011**, *133*, 9224-9227.

157   Braga, D.; Grepioni, F.; Lampronti, G. I.; Maini, L.; Turrina, A. *Cryst. Growth Des.* **2011**, *12*, 5621-5627.

Cocrystallization of nutraceuticals

Abhijeet S. Sinha,[†] Anita R. Maguire,[§] and Simon E. Lawrence[†]*

Nutraceuticals are attractive as coformers due to their ready availability, known pharmacological profile and natural origin. This review details the structural data of nutraceuticals in pure form and in their multicomponent materials, identifies the persistent supramolecular features present and highlights studies which have favorably altered the physicochemical properties of nutraceuticals through cocrystallization.